7-17-1966

Convective heat transfer coefficients and pressure drop data from multi-start helical fin tubes in longitudinal flow.

Leonard S. Thomas
University of Windsor

CONVECTIVE HEAT TRANSFER COEFFICIENTS AND PRESSURE DROP DATA FROM MULTI-START HELICAL FIN TUBES IN LONGITUDINAL FLOW

A Thesis

Submitted to the Faculty of Graduate Studies Through the Department of Mechanical Engineering in Partial Fulfillment of the Requirements for the Degree of Master of Applied Sciences at the University of Windsor

by

Leonard S. Thomas

Windsor, Ontario, Canada

1966

ABM 2309

1354.78

ABSTRACT

The effects of fin spacing (Pitch) and radial clearance (R_c) between the fin tips and the outer annulus wall, on heat transfer and pressure drop from four start helical fin tubes in steady turbulent annular flow have been investigated. The fin tubes were fabricated from an aluminum alloy and each had the same trapezoidal fin profile. The heat flux was generated electrically within the fin tube and was held at a constant 5.0 kilowatts (1.66 kilowatts/linear foot of fin tube) for all test runs. Atmospheric air flowing longitudinally within the annular test section was utilized as the cooling fluid.

The results show the heat transfer data could be correlated in terms of the conventional parameters N_{Nu} , N_{Re} , N_{Pr} and two additional geometric variables N_{G1}, N_{G2} which allowed for the variation of (Pitch) and (R_c). When the log mean temperature difference ΔT_{lm} , based on the inlet and outlet temperature differences was used, the following correlation equation may be applied:

$$N_{Nu} = 0.058 (N_{Re})^{0.8} (N_{Pr})^{0.4} (N_{G2})^{0.625} (N_{G1})^{0.661} \qquad \text{Eq. (5-2)}$$

When the temperature difference was non-linear between the inlet and outlet, the following correlation based on an area weighted temperature difference $\Delta T'_{lm}$ adequately correlated the results:

$$N'_{Nu} = 0.287 (N_{Re})^{0.634} (N_{Pr})^{0.4} (N_{G2})^{-0.25} (N_{G1})^{-0.414} \qquad \text{Eq. (5-4)}$$

where 1. $10000 < N_{Re} < 43000$

2. $N_{Pr} = 0.692$

3. $N_{G1} = \frac{\text{Pitch}}{\text{Equivalent Diameter}}$

$0.625 < \text{pitch} < 1.400$, inches

4. $N_{G2} = \frac{\text{Radial clearance}}{\text{Equivalent Diameter}}$

$0.0 < \text{Radial clearance} < 0.375$, inches

The experimental determination of the fin efficiency (ϕ) for the trapezoidal fin profile was found to be in good agreement with the results of other investigators in the range covered.

The pressure drop characteristics of the annular test section were found to be adequately expressed by the Fanning friction factor (f) and for any one fin tube-annulus arrangement, were relatively independent of the Reynolds Number.

ACKNOWLEDGEMENTS

The author wishes to express his graditude to the following: Professor G. B. Babiy for his supervision throughout this work, to Dr. A. A. Nicol for his many helpful suggestions, to Messrs. Peter K. C. Tu, R. A. Myers, and Otto Brudy for their technical assistance.

Acknowledgement is also due the National Research Council and the Mechanical Engineering Department, University of Windsor for their financial support.

TABLE OF CONTENTS

LIST OF FIGURES

NOTATION

a_1 = Constant

A_n = Free flow area perpendicular to axis of fin tube, ft^2

A_T = Total heat transfer surface area of fin tube, ft^2

b_1 b_2 b_3 = Exponents

Cp = Specific heat at constant pressure, Btu/lb ^oF

d = Tube diameter, ft

d_1 = Outside diameter of inner tube of an annulus, ft

d_2 = Inside diameter of outer tube of an annulus, ft

DA = Diameter of annulus, ft

DR = Diameter of fin tube at root of fins, ft

D_e = Equivalent diameter = $d_2 - d_1$, ft

D_E = Equivalent diameter = $4 \frac{A_n}{P_n}$, ft

ft = length, feet

G = Mass velocity = ρV_m lb/hr ft^2

g_c = Gravitational constant = $4.17 \times 10^8 \frac{lb}{lbf} \times \frac{ft}{hr^2}$

h = Local heat transfer coefficient Btu/ft^2 hr ^oF

h_m = Average heat transfer coefficient of heated fin tube surface, Btu/hr ft^2 ^oF

h_m' = Average heat transfer coefficient based on segmented (LMTD) Btu/hr ft^2 ^oF

hr = Time, hour

k = Thermal conductivity Btu/ft hr ^oF

L = Length, foot

lb = Pound mass

lbf = Pound force

ln = Logarithm to base e

M = Mass flow rate lb/hr

p = Static pressure lbf/ft^2

$\bar{p}$ = Average of two pressures

P = Pitch of fins, ft

P_n = Total wetted perimeter normal to fin tube axis, ft

q = Heat flow, Btu/hr

r = Radius of tube, ft

R = Gas constant, ft lbf/lb ^{o}R

R_c = Radial annular clearance, ft

T = Temperature, ^{o}F

$\overline{T}$ = Average of two temperatures, ^{o}F

T_b = Bulk temperature ^{o}F

T_{lm} = (LMTD) = log mean temperature difference, ^{o}F

T'_{lm} = $(LMTD)'$ = Segmented log mean temperature difference, ^{o}F

T_{SA} = Average surface temperature, ^{o}F

T_{SR} = Surface temperature at fin root, ^{o}F

T_{ST} = Surface temperature at fin tip, ^{o}F

T_{wall} = Temperature of tube wall, ^{o}F

V = Velocity, ft/hr

V_m = Mean velocity = $\dfrac{M}{\rho A_n}$, ft/hr

Z = Fin height, ft

W = Average fin thickness, ft

NOMENCLATURE

GREEK SYMBOLS

ϕ	=	Fin efficiency
Δ	=	Difference of two values
μ	=	Dynamic viscosity, lb/ft hr
ρ	=	Density, lb/ft^3
ψ	=	Functional relation
τ	=	Shear stress, lbf/ft^2 hr

DIMENSIONLESS NUMBERS

Nusselt Number, $N_{Nu} = \frac{h_m d}{k}$

Prandtl Number, $N_{Pr} = \frac{\mu Cp}{k}$

Reynolds Number, $N_{Re} = \frac{\rho V d}{\mu} = \frac{d G}{\mu}$

Stanton Number, $N_{St} = \frac{h_m}{Cp\ G}$

$N_{G1} = \frac{P}{D_E}$

$N_{G2} = \frac{(DA - DR)/2}{D_E}$

Fanning friction factor, $f = \frac{\Delta P\ D_E\ \rho\ g_c}{2L\ G^2}$

Friction factor, $f' = \frac{\Delta P\ D_E\ \rho\ g_c}{2L\ G^2} - \left[\frac{T_5 - T_1}{\bar{T}}\right]$

CHAPTER I

INTRODUCTION

The object in the design of convective heat transfer equipment is to achieve the maximum heat release from a source at a given temperature with an optimum economic balance between the surface area and pressure drop requirements. When the design criteria place limiting factors on the regime of flow and the selection of heat transfer media, extended surfaces such as fins often enable the designer to meet the specification imposed on him.

For example, in the design of a gas-cooled nuclear reactor the process of heat removal from the reactor cannot be dealt with as an isolated problem, but must be closely integrated with the nuclear, metallurgical, and structural design. The greatest difference between the heat transfer problem in a reactor and that occurring in most industrial applications is the limitation imposed by nuclear design. Some of these limitations are the disposition of the fuel in the coolant channel, the size of the channel, and the nature of the material that may be used to form the extended surfaces.

Recent interest in reactor design has generated some information on flow of gases over helical surfaces in annular passages. However, little information is available for the case where the annular gap between the fins and the outer tube wall is very small. The applicable parameters of annular flow, such as the equivalent diameter, are not universally agreed upon and the results of different investigators cannot always be correlated.

Therefore the object of this investigation is to provide information on the heat transfer and pressure drop occurring from four start helical fin tubes in annular passages during turbulent steady flow where the pitch of the fins and the clearance between the fin tips and outer wall of the annulus are both varied.

CHAPTER II

LITERATURE SURVEY

The term convective heat transfer usually refers to the combined mechanism of heat and momentum transfer. In the turbulent regime of flow there exists a boundary layer of fluid over the heated surface which transfers heat by conduction, convection and radiation. The actual contribution of each mode of heat transfer is so complex that only a few exact restricted analytical solutions describing these phenomena have been found to date. Therefore, the purpose of this chapter is to discuss some of the results of past theoretical and empirical investigations pertinent to the turbulent flow of fluids over heated surfaces in confined passages.

A. Turbulent Heat Transfer Inside Smooth Circular Tubes

Although the geometry of a circular tube appears simple the lack of knowledge about the velocity and temperature distribution within the fluid limits the analytical approach. Early investigators such as Reynolds[1] and Prandtl[2] made use of the analogy between heat and momentum transfer to obtain solutions for the heat transfer coefficient. However, these solutions are restricted to a narrow range of variables because of the necessary assumptions in their derivations. Semi-empirical solutions utilizing dimensional analysis and experimental data have been developed which yield fair accuracy for a wide range of variables. Dittus and Boelter[3] correlated the results of thirteen investigators and proposed the following equation:

$$\left[\frac{h_m\, d}{k}\right] = 0.023 \left[\frac{\rho V_m\, d}{\mu}\right]^{0.8} \left[\frac{Cp\ \mu}{k}\right] \qquad \text{Eq. (2-1)}$$

where

1. Fluid properties evaluated at arithmetic mean bulk temperature, Tb
2. d = inside dia. of tube
3. L = length of tube
4. $\left[\frac{\rho V_m\, d}{\mu}\right] > 10000$
5. $0.7 < \left[\frac{Cp\ \mu}{k}\right] < 100$
6. n = 0.3 for cooling, 0.4 for heating
7. $L/d > 60$

Colburn[4] further proposed a correlation from his work using the Stanton Number instead of the Nusselt Number:

$$\left[\frac{h_m\ Cp}{G}\right] = 0.023 \left[\frac{Cp\ \mu}{k}\right]_{T_{0.5}}^{-\frac{2}{3}} \left[\frac{G\ d}{\mu}\right]_{T_{0.5}}^{-0.2} \qquad \text{Eq. (2-2)}$$

where 1. Fluid properties, except Cp, evaluated at film temperature, $T_{0.5}$:

$$T_{0.5} = \left[\frac{T_{wall} + T_b}{2}\right]$$

Cp evaluated at bulk temperature

2. $\left[\frac{G\ d}{\mu}\right] > 10000$

3. $0.7 < \left[\frac{Cp\ \mu}{k}\right] < 160$

4. $L/d > 60$

B. Turbulent Heat Transfer in Smooth Annuli

For the case of smooth concentric tubes forming annuli, where heat is transferred from the surface of the inner tube to a fluid confined in the outer tube, an extension of Equation (2-1) was proposed by Wiegand[5]. However, an additional term was added to account for the geometry of the annulus. This was expressed as a ratio of the tube diameters comprising the system.

$$\left[\frac{h_m d_e}{k}\right] = 0.023 \left[\frac{d_e G}{\mu}\right]^{0.8} \left[\frac{Cp\ \mu}{k}\right]^{0.4} \left[\frac{d_2}{d_1}\right]^{0.45} \qquad \text{Eq. (2-3)}$$

where 1. Fluid properties evaluated at bulk temperature, T_b

2. d_1 = inner tube outside dia.

d_2 = outer tube inside dia.

3. $d_e = (d_2 - d_1)$ = equivalent diameter

4. $\left[\frac{d_e G}{\mu}\right] > 10000$

Monrad and Pelton[6] from their experimental work proposed the following equation:

$$\left[\frac{h_m d_e}{k}\right] = 0.020 \left[\frac{d_e G}{\mu}\right]^{0.8} \left[\frac{Cp\ \mu}{k}\right]^{\frac{1}{3}} \left[\frac{d_2}{d_1}\right]^{0.53} \qquad \text{Eq. (2-4)}$$

where the conditions are similar as described in Equation (3).

The exact effects of the entrance section of annular configurations on the heat transfer have not been fully established. The work of Miller, Byrnes, and Benforado[7] while agreeing with Equation (2-3) showed that the velocity profile was established in a length $20[d_e]$ and the Nusselt Number was constant in a length $4[d_e]$ from the annulus entrance.

C. Turbulent Heat Transfer in Modified Annuli Containing Fin Tubes

Gunter and Shaw[8] and de Lorenzo and Anderson[9] conducted heat transfer experiments on commercial double pipe heat exchangers

containing continuous and non-continuous straight longitudinal fins. The term non-continuous refers to fin tubes which had radial slots cut into the fin surface to promote turbulent mixing of the fluid. Their results were correlated by Equation (2-2) with the addition of the term $\left[\frac{\mu}{\mu_w}\right]^{-0.14}$ on the right hand side, where μ and μ_w are the viscosities of the fluid evaluated at the bulk and average fin surface temperatures respectively. This term was introduced to account for the influence of temperature on viscosity, predominant in hydrocarbon fluids. In addition their work showed that the non-continuous fins displayed higher heat transfer coefficients than the continuous fins. This was attributed to smaller build up of the thermal boundary layer on the non-continuous fins.

Knudsen and Katz[10] conducted heat transfer experiments on six different single start helical fin tubes using water as the cooling fluid. From dimensional analysis they showed that the heat transfer could be correlated by an expression similar to Equation (2-1) with the addition of dimensionless groups describing the geometry of the system. For their work, they essentially held all geometry constant except the fin height and spacing between adjacent fins and proposed the following correlation:

$$\left[\frac{h_m d_e}{k}\right] = 0.039 \left[\frac{G d_e}{\mu}\right]^{0.87} \left[\frac{Cp\ \mu}{k}\right]^{0.4} \left[\frac{P}{d_e}\right]^{0.4} \left[\frac{Z}{d_e}\right]^{-0.19}$$

Eq. (2-5)

where 1. P = Pitch = Spacing between adjacent fins

2. Z = fin height

3. $1 < Z/P < 2$

4. Fluid properties evaluated at bulk temperature, T_b

Chant[11] performed heat transfer experiments on a configuration representing a double pipe heat exchanger in which the inner element consisted of a three-start helical fin tube with a pitch of 0.88 inch. Air was used as the cooling fluid. The clearance between the outer wall and the fin tip was varied in four increments giving a range of 0.187 to 1.517 inches. The results of his work showed that an equivalent diameter based on d_e did not adequately correlate his findings, instead he proposed the following relation for the equivalent diameter:

$$D_E = 4\left[\frac{A_n}{P_n}\right] \qquad \text{Eq. (2-6)}$$

where A_n = Flow area perpendicular to the axis of the fin tube.

P_n = Wetted perimeter of flow passage perpendicular to the axis of the fin tube.

In addition he expressed the correlation of his heat transfer findings as:

$$\left[\frac{h_m D_E}{k}\right] = 0.044 \frac{\left[\frac{G D_E}{\mu}\right]^{0.8} \left[\frac{D_E}{Do}\right]^{0.8} \left[\frac{Cp\ \mu}{k}\right]^{0.4}}{\left[\frac{P}{D_E}\right]^{0.4} \left[\frac{D_A}{Dr}\right]^{0.8}} \qquad \text{Eq. (2-7)}$$

where 1. Do = Outside diameter of fin tube

2. Dr = Root diameter of fin tube

3. D_A = Inside diameter of outer tube

4. P = Pitch = space between adjacent fins

5. Properties of the fluid evaluated at the mean temperature difference between the fin tube and the fluid.

D. Heat Transfer From Extended Surfaces

The use of extended surfaces such as fins* on a circular tube, is usually thought of as an aid to increase the heat transfer from the tube. However, the possibility of an actual reduction in the heat transfer must also be considered. This is due to the fact that the heat transfer is dependent on the temperature difference between the fin surface and the bulk temperature of the fluid surrounding the fin. As the fin length is traversed the temperature difference between the fin and the fluid may decrease more rapidly than the surface area increases. The temperature gradient in the fin is a complex function of the following variables:

1. Thermal conductivity of the fin material.

2. Geometry of the fin profile.

3. Heat transfer coefficient of the fin surface.

There are two criteria generally used in rating the performance of fins. The first is called fin effectiveness and is equal to the ratio of the heat transferred through the fin root area to that which would be transferred from the same root area if the

* (The term fin is commonly used as a concise generic term for all forms of extended surfaces.)

fin were not present and if the root area temperature remained unchanged. The second criteria is called the fin efficiency and is equal to the ratio of the heat transferred from a fin of finite thermal conductivity to the heat transferred from an identical surface of infinite thermal conductivity. The fin efficiency definition is a more realistic measure of the fin performance as the root temperature in the fin effectiveness definition cannot be expected to remain unchanged in the actual case.

Gardner[12] showed that the temperature gradient equation derived for any form of extended surface can be reduced to a generalized Bessel equation, provided the cross-sectional area varies as some power of the distance measured from a given zero point in the direction normal to the base surface. The results of his analytical treatment of the problem are presented in the form of curves. Of the assumptions used in deriving his results, the two that appear most likely to deviate from actual conditions are:

1. A constant heat transfer coefficient over the entire extended surface.
2. Uniform fluid temperature surrounding the extended surface.

These assumptions are invalid for longitudinal flow over transverse fins. Recognizing this, Fortescue and Hall[13] correlated their work by using the Stanton Number as a heat transfer parameter. They expressed their results as follows:

$$N_{St} = \text{f}\,[N_{Re}\ (kg/km)] \qquad \text{Eq. (2-8)}$$

where k_g = thermal conductivity of cooling fluid

k_m = thermal conductivity of fin material

This method of correlating the heat transfer appears adequate if the fin geometry remains constant. However, when correlating the effects of fin geometry and material the fin efficiency, while not rigorously accurate, is recommended as the dimensionless parameter in determining the heat transfer coefficient.

E. Friction Factors in Modified Annuli

As for the case of heat transfer in modified annuli, the friction factor is also a complex function of many variables. Numerous studies on friction losses occurring during turbulent flow have indicated that the friction losses are proportional to the kinetic energy of the fluid per unit volume, the area of the solid surface in contact with the fluid, and the viscosity of the fluid. In general the Fanning friction factor (f) is used and is determined from the measured pressure drop.

$$f = \left[\frac{\Delta p \; D_E \; g_c}{2L \rho V_m^2}\right] \qquad \text{Eq. (2-9)}$$

where:

Δp = pressure drop over length, L

D_E = equivalent diameter

V_m = mean velocity of fluid

For turbulent flow in annuli constructed from concentric smooth tubes Knudsen and Katz[14] averaged the results of a number of empirical investigations and proposed:

$$f = 0.076 \left[\frac{d_e \; G}{\mu}\right]^{-0.25} \qquad \text{Eq. (2-10)}$$

where 1. d_e = as defined in Equation (2-3)

2. $3000 < N_{Re} < 10^6$

However some of the experimental results were observed to deviate as much as 35% from Equation (2-9).

Braun and Knudsen[15] determined isothermal friction factors for water flowing in modified annuli. They constructed fin tubes by placing circular metal disks on a solid rod with the distance between the disks varied by tubular spacers. The outside tube diameter of the annulus was held constant for all tests. Their results showed that for a constant fin height the friction factor for a fin tube increases with increasing fin spacing up to a certain point and then decreases as the fin spacing is further increased. The equivalent diameter term was defined as the difference between the outer annulus tube wall diameter and the outside diameter of the inner fin tube. Further, their results showed that for each fin tube tested a seperate friction factor versus Reynolds Number curve was obtained. These curves are similar to the classical work of Nikuradse[16] in his study of artifically roughened pipes.

Cunningham and Slack[17] determined friction factors for carbon dioxide gas and air flowing over multi-start helical fin tubes mounted concentrically in round passages. They showed that the friction factor was independent of Reynolds Number for their work and correlated their results as follows:

$$f = 0.00086 + 0.303 \left[\frac{Do}{\ell \sqrt{n}}\right] \qquad \text{Eq. (2-11)}$$

where

1. Do = Outside diameter of fin tube, inches
   $1.8 < Do < 3.0$
2. ℓ = Helical lead of fin tube, inches
   $12 < \ell < 36$
3. n = number of fins
   $30 < n < 48$
4. $7 \times 10^4 < N_{Re} < 3 \times 10^5$

Fortescue and Hall [13] performed friction factor measurements on a set of heated, straight, longitudinally finned tubes mounted concentrically in a 4.0 inch dia. channel. The fin height was varied from 0.0. to 1.0 inches, and the number of fins varied from 0 to 16, all equally spaced circumferentially about the tube. The fins were made from an aluminum alloy and all were 0.020 inch thick. They noted that the correlation of their findings was unaffected by a change in fin height for the range tested and expressed their results in the form:

$$f = [0.083]^{-0.026n} \left[\frac{G\, D_E}{\mu}\right]^{-0.2} \qquad \text{Eq. (2-12)}$$

where

1. n = number of fins
2. D_E = as defined in Equation (2-6)
3. Properties of the cooling fluid evaluated at the mean temperature difference between the fin tube surface and the coolant fluid. Air and CO_2 at 100 psig were the fluids.
4. Radial clearance between fin tips and channel wall ranged between 0.0 to 1.0 inches.

CHAPTER III

THEORETICAL AND EMPIRICAL CONSIDERATIONS

The results of other investigations pertinent to the turbulent flow of fluids in modified annuli have been discussed in Chapter II. This chapter deals with the theoretical and empirical relations used in the analysis of the present investigation.

A. Heat Transfer

Since the fin tube and outer annulus combinations used in this investigation are similar to a double pipe heat exchanger configuration, the same method of analysis for determining the heat transfer performance may be applied. The rate of heat transfer from the heated fin tube surface to the coolant air flowing past may be expressed as:

$$q = \int_0^{A_T} h \, \Delta T \, dA_T \qquad \text{Eq. (3-1)}$$

where q = heat transfer rate, Btu/hr.

h = local heat transfer coefficient, Btu/hr ft^2 ^oF

ΔT = local temperature difference between the average air temperature and the average surface temperature, ^oF

A_T = heat transfer surface area of fin tube, ft^2

Assuming a uniform or constant heat transfer coefficient (h_m) to exist over the entire heat transfer surface of the fin tube, Equation (3-1) may be written:

$$q = h_m \int_0^{A_T} \Delta T \, dA_T \qquad \text{Eq. (3-2)}$$

In determining the temperature difference between the air and heat transfer surface area of the fin tube, the temperature gradients at any cross-section in both the air and the fin tube surface must be considered. The average air temperature at the cross-section may be evaluated by the bulk temperature (T_b). This is defined as the average temperature of a quantity of air passing a given cross-section per unit time. For an annular corss-section the bulk temperature may be expressed as:

$$T_b = \frac{\int_{r_i}^{r_o} \rho Cp \; T \; V \; r \; dr}{\int_{r_i}^{r_o} \rho Cp \; V \; r \; dr} \qquad \text{Eq. (3-3)}$$

where ρ = Density of air

Cp = Specific heat of air at constant pressure

V = Velocity of air at radius r

T = Temperature of air at radius r

r_i = DR/2

r_o = DA/2

Referring to Figure No. 1, it can be seen that there will exist a radial temperature gradient on the fin tube surface at any cross-section due to the thermal resistance of the fin tube material. The exact location of the average surface temperature is difficult to obtain from direct measurement. However, it is convenient to measure the surface

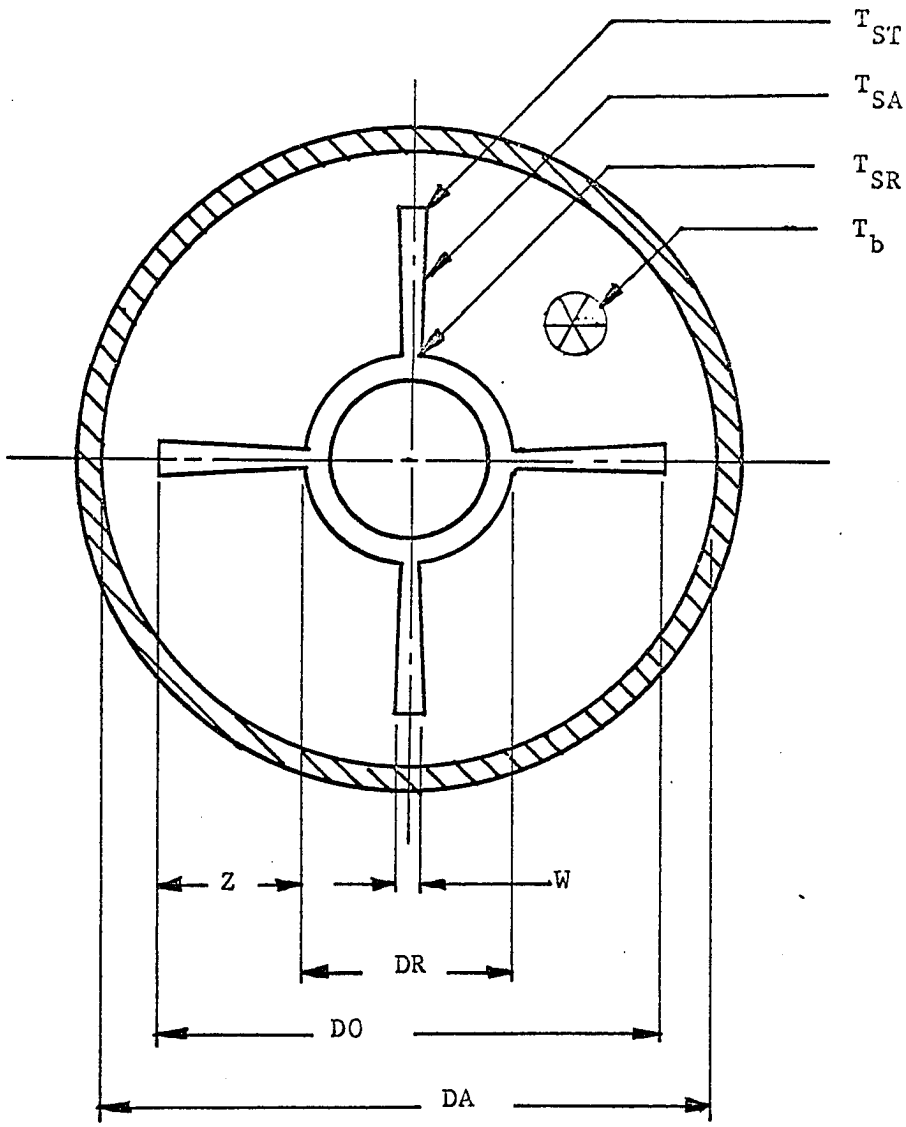

DA = Annulus inside diameter

DO = Outside diameter of fintube

DR = Diameter of fin tube at root of fins

W = Average fin thickness

Z = Fin height

T_b = Bulk temperature of air

T_{SA} = Average Surface temperature of fin tube

T_{SR} = Surface temperature of fin tube at root of fin

T_{ST} = Surface temperature of fin at tip of fin

FIGURE NO: 1 CROSS-SECTIONAL VIEW OF FIN TUBE AND ANNULUS PERPENDICULAR TO AXIS OF FIN TUBE

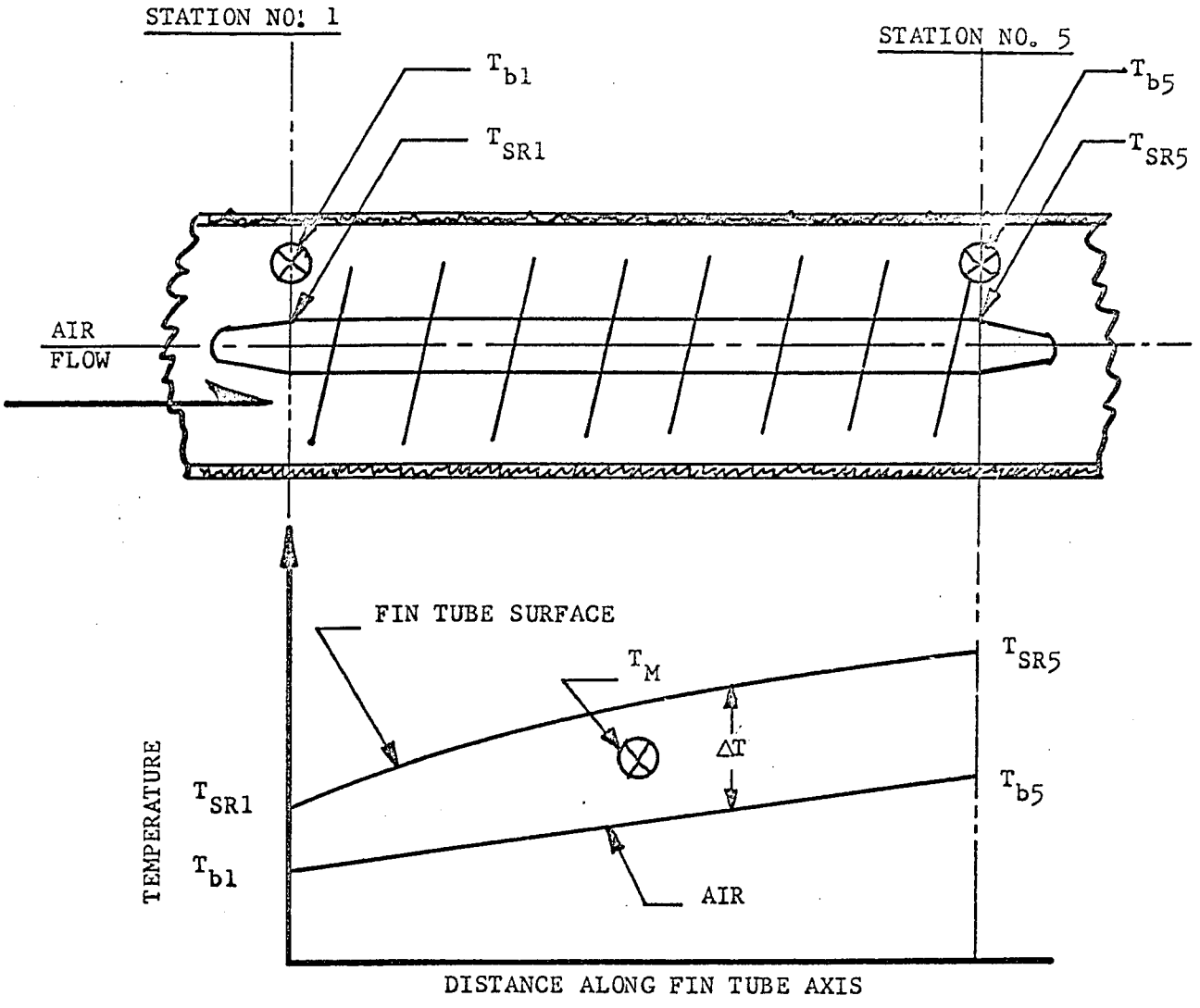

T_{SR1} = Temperature of fin tube surface at fin root, Station No. 1

T_{SR5} = Temperature of fin tube surface at fin root, Station No. 5

T_{b1} = Bulk temperature of air at Station No. 1

T_{b5} = Bulk temperature of air at Station No. 5

T_M = Mean temperature difference between fin surface and air.

FIGURE NO. 2 FIN TUBE SURFACE AND AIR TEMPERATURE DISTRIBUTION ALONG FIN TUBE AXIS

temperature of the fin tube at the root of the fin. Thus to apply equation (3-1) to a surface with a radial temperature gradient, a relation is required between the heat transfer rate at the fin root and the heat transfer rate at the point of average surface temperature. This relationship is provided by the fin efficiency term (ϕ) and is defined as the ratio of the heat transferred from a fin of finite thermal conductivity to the heat transferred from an identical fin of infinite thermal conductivity.

that is:

$$\phi = \frac{\int_0^{A_F} h\,(T_{SA} - T_b)\,dA_F}{\int_0^{A_F} h\,(T_{SR} - T_b)\,dA_F} \qquad \text{Eq. (3-4)}$$

When h is assumed to be constant (h_m) over the entire fin, then Equation (3-4) may be written:

$$\phi = \frac{h_m A_F (T_{SA} - T_b)}{h_m A_F (T_{SR} - T_b)} \qquad \text{Eq. (3-5)}$$

$$\phi = \left[\frac{(T_{SA} - T_b)}{(T_{SR} - T_b)}\right] \qquad \text{Eq. 3-6)}$$

Once the fin efficiency is found the effective heat transfer surface area may be determined from the relation:

$$A_T = A_t + \phi A_F \qquad \text{Eq. (3-7)}$$

where A_t = surface area of tube

A_F = surface area of fins

Referring to Figure No. 2 it can be seen that there also exists a temperature gradient along the axis of the fin tube. The gradient (ΔT) is not constant and may be evaluated by the log-mean temperature difference (LMTD) method. Hence (ΔT) from Equation (3-1) may be written:

$$\Delta T = \Delta T_{lm} = \frac{[(T_{SR5} - T_{b5}) - (T_{SR1} - T_{b1})]}{\ln \left[\frac{(T_{SR} - T_{b5})}{T_{SR1} - T_{b1})} \right]} \qquad \text{Eq. (3-8)}$$

$$\Delta_{T_{lm}} = \frac{(\Delta T_5 - \Delta T_1)}{\ln \left[\frac{\Delta T_5}{\Delta T_1} \right]} \qquad \text{Eq. (3-9)}$$

Having accounted for the temperature gradients in the radial and axial direction, Equation (3-2) may be rewritten:

$$h_m = \frac{q}{\Delta T_{lm} (A_t + \phi A_F)} \qquad \text{Eq. (3-10)}$$

The effects of the operating variables on the heat transfer coefficient can be correlated from dimensional analysis, e. g., see References (3, 10, 17, 18). Problems dealing with forced convection have been shown to be governed by an equation of the form:

$$\psi_1 (N_{Re} , N_{Pr} , N_{Nu} , N_{G1} , N_{G2} \ldots . N_{Gn}) = 0 \qquad \text{Eq. (3-11)}$$

where

1. $N_{Re} = \left[\frac{d_e G}{\mu}\right]$ = Reynolds Number

2. $N_{Pr} = \left[\frac{Cp\ \mu}{k}\right]$ = Prandtl Number

3. $N_{Nu} = \left[\frac{h_m d_e}{k}\right]$ = Nusselt Number

4. $N_{G1} \ldots . N_{Gn}$ = Dimensionless grouping of variables describing the geometry of the heat transfer system.

For this investigation all geometry of the system remained constant except the following:

1. Pitch of fins, i.e., spacing between adjacent fins.
2. Radial clearance between the fin tips and the annulus wall.

Since these geometric variables contain the units of length, they can be made dimensionless by division with the characteristic length term, the equivalent diameter (d_e). For an annular configuration constructed from smooth concentric tubes, the equivalent diameter may be expressed as:

$$d_e = \left[\frac{4\ (\text{Flow area})}{\text{Wetted perimeter}}\right] \qquad \text{Eq. (3-12)}$$

$$= \frac{\pi\ (d_2^2 - d_1^2)}{\pi\ (d_2 + d_1)} \qquad \text{Eq. (3-13)}$$

$$= \left[d_2 - d_1\right]$$

where d_1 = inner tube outside diameter

d_2 = outer tube inside diameter

However this expression for the equivalent diameter is invalid for fin tubes in modified annuli when the limiting case of $\left[d_2 = d_1\right]$ is present as in this investigation. Therefore a new definition based on the work of Chant[11] is proposed:

$$D_E = \left[\frac{4(A_n)}{P_n}\right] \qquad \text{Eq.(2-6)}$$

Hence the geometric variables of pitch and radial clearance may be written:

$$N_{G1} = \left[\frac{P}{D_E}\right] \qquad \text{Eq. (3-15)}$$

$$N_{G2} = \left[\frac{(DA - DR)\ /2}{D_E}\right] \qquad \text{Eq. (3-16)}$$

where 1. P = Pitch of fins

2. DA, DR = dimensions of fin tube as described in Fig. No. 1

Since the Nusselt Number contains the desired heat transfer term (h_m), Equation (3-11) may be rewritten by the functional relation:

$$N_{Nu} = \psi_2 [N_{Re} , N_{Pr} , N_{G1} , N_{G2}] \qquad \text{Eq. (3-17)}$$

From Buckingham's Pi Theorem, Equation (3-17) may be rewritten:

$$N_{Nu} = a_1 (N_{Re})^{b1} (N_{G1})^{b2} (N_{G2})^{b3} (N_{Pr})^{b4} \qquad \text{Eq. (3-18)}$$

Equation (3-18) is similar to the Dittus-Boelter Equation, Equation (2-1), and since the Prandtl Number of air does not vary appreciably for the range of pressures and temperatures encountered in this investigation, the exponent (b4) may be assigned the value of 0.4. Thus rewriting Equation (3-18):

$$\frac{N_{Nu}}{[N_{Pr}]^{0.4}} = a_1 (N_{Re})^{b1} (N_{G1})^{b2} (N_{G2})^{b3} \qquad \text{Eq. (3-19)}$$

where the constant (a_1) and the exponents (b1, b2, b3) are determined from experimental data and multiple linear regression techniques derived from statistical analysis.*

* (A complete and detailed treatment of regression techniques may be found in Reference No. 19, pp. 208 - 211).

B. Friction Factor

As the air flows axially through the annular test section between Station No. 1 and Station No. 5 (see Figure No. 3), it will experience a pressure drop. This pressure drop is the result of two factors: first, as a result of the drag forces on the fin tube heat transfer surface and annulus wall; second, as a result of the acceleration of the air as it passes through the annular test section. This acceleration will occur even in a circular passage of uniform diameter since the air expands as it is heated. For liquids the acceleration is small and may be neglected, however for gases it may, depending on the temperatures encountered, contribute significantly to the overall pressure drop.

The pressure drop in the axial direction may be calculated by application of the equations of continuity and momentum. The continuity equation may be written:

$$\rho V_m A_n = \text{Constant} = M \qquad \text{Eq. (3-20)}$$

where 1. ρ = density of air

2. V_m = mean velocity of air

3. A_n = Free cross-sectional flow area perpendicular to the axis of the fin tube.

The equation of motion, for an element of annular test section dx long, may be written:

Pressure forces on ends of element = drag forces on surface +

+ change in momentum flux over length, dx

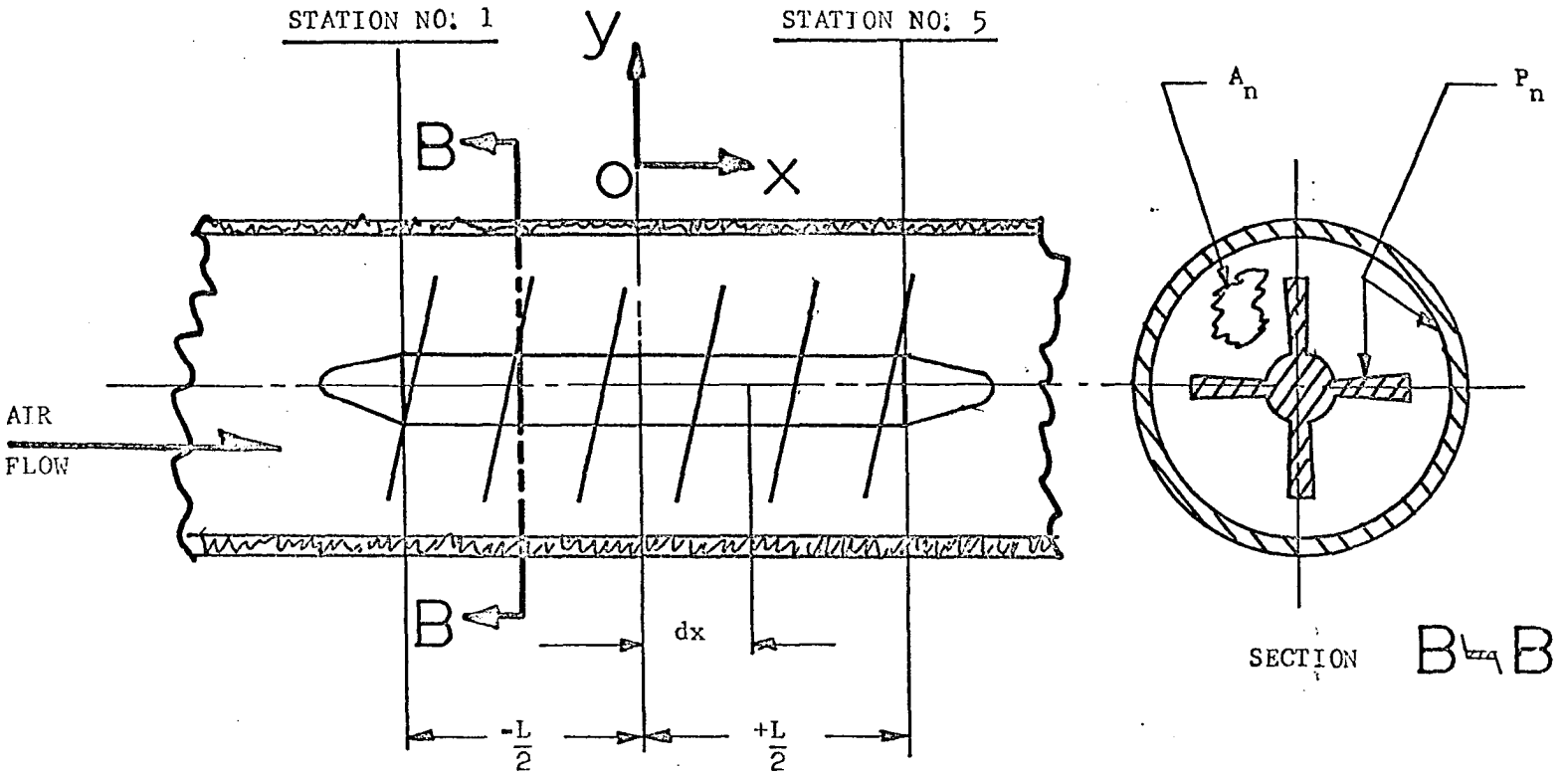

A_n = Free cross-sectional flow area perpendicular to axis of fin tube.

P_n = Wetted perimeter of fin tube and annulus perpendicular to axis of fin tube.

FIG: NO. 3 DIAGRAM OF FIN TUBE AND ANNULUS DESCRIBING THE NOMENCLATURE FOR FRICTION FACTOR CALCULATION

that is

$$-A_n\, dp = \tau\, P_n\, dx + \rho\, A_n\, V_m\, dV_m \qquad \text{Eq. (3-22)}$$

since

$$\tau = 1/2\left[\rho\, V_m^2\right] f' \qquad \text{Eq. (3-23)}$$

and

$$P_n = \left[\frac{4\, A_n}{D_E}\right] \qquad \text{Eq. (3-24)}$$

then

$$-dp = f'\left[\frac{\rho V_m^2}{2}\right]\left[\frac{4}{D_E}\right] dx + \rho V_m\, dV_m \qquad \text{Eq. (3-25)}$$

where

1. dp = pressure increase in the axial direction of the annular test section
2. D_E = equivalent diameter, Eq. (2-6)
3. P_n = total wetted perimeter of fin tube surface and annulus perpendicular to the axis of the fin tube
4. τ = drag force per unit area
5. f' = dimensionless friction factor

Since the cross-sectional flow area is uniform in the axial direction and $(\rho\, V_m)$ is constant, Equation (3-22) may be written:

$$(p_1 - p_5) = 1/2\left[\frac{M}{A_n}\right]^2\left[\frac{4}{D_E}\right]\int_{-L/2}^{+L/2}\frac{f'}{\rho}dx + \frac{M}{A_n}\left[(V_{m5} - V_{m1})\right] \qquad \text{Eq. (3-26)}$$

Where subscripts 1 and 5 refer to the inlet and outlet conditions of the air, respectively.

For turbulent flow the friction factor is proportional to $(Nre)^{-0.25}$ (Reference No. 14). The viscosity is the only factor that influences the Reynolds Number, since the geometry of the system is constant in the axial direction. For a gas such as air, the viscosity is observed to change slowly with temperature. Hence, the change in the friction factor in the axial direction will be very small and a value approximate to the mid-point at X = 0 may be used. Further, as in the case of viscosity, the air density will be more influenced by temperature than the pressure. Assuming pressure changes are negligible and using the pressure at the mid-point of the fin tube, X = 0, for calculating the density, then:

$$\bar{p} = (P_1 + P_5)/2 \qquad \text{Eq. (3-27)}$$

but

$$\rho = \frac{p}{RT} \qquad \text{Eq. (3-28)}$$

where
1. ρ = density of air
2. p = pressure of air
3. R = Gas Constant = 53.35 ft lbf/lb $^{\circ}$F
4. T = absolute temperature of air

evaluating the term

$$\int_{-L/2}^{+L/2} \frac{1}{\rho}\, dx = \left(\frac{R}{\bar{p}}\right) \left[\frac{T_5 + T_1}{2}\right] L \qquad \text{Eq. (3-29)}$$

but

$$\bar{T} = (T_5 + T_1)/2 \qquad \text{Eq. (3-30)}$$

then Eq. (3-29) may be written:

$$\left[\frac{R}{\bar{p}}\right]\left(\frac{T_5 + T_1}{2}\right) L = \frac{R\,\bar{T}\,L}{\bar{p}} \qquad \text{Eq. (3-31)}$$

also

$$\left[\frac{M}{A_n}\right]\left(V_{m5} - V_{m1}\right) = \left[\frac{M}{A_n}\right]^2 \left(\frac{1}{\rho_5} - \frac{1}{\rho_1}\right) = \left[\frac{M}{A_n}\right]^2 \frac{R}{\bar{p}} \left[T_5 - T_1\right]$$

Eq. (3-32)

rewritting Eq. (3-26) in terms of theabove expression:

$$P_1 - P_5 = \left[\frac{M}{A_n}\right]^2 \frac{R}{\bar{p}} \left[\frac{2 f' \bar{T}}{D_E} + T_5 - T_1\right] \qquad \text{Eq. (3-33)}$$

but from the relation

$$\bar{p} = R\,\bar{\rho}\,\bar{T} \qquad \text{Eq. (3-34)}$$

Eq. (3-33) may be rewritten:

$$\Delta p = \left[p_1 - p_5 \right] = \frac{1}{\bar{\rho}} \left[\frac{M}{A_n} \right]^2 \left[\frac{2 f' L}{D_E} + \frac{T_5 - T_1}{\bar{T}} \right]$$

Eq. (3-35)

For moderate air temperatures the term $\left[\frac{T_5 - T_1}{\bar{T}} \right]$ may be neglected and the resulting equation is similar to the expression for the Fanning friction factor.

$$\Delta p = \frac{1}{\bar{\rho}} \left[\frac{M}{A_n} \right]^2 \left[\frac{2 f L}{D_E} \right]$$

Eq. (3-36)

substituting for $\left[\frac{M}{A_n} \right] = \bar{\rho} V_m = G$

then

$$f = \left[\frac{\Delta p \ D_E \ \bar{\rho} \ g_c}{2 L G^2} \right]$$

Eq. (3-37)

CHAPTER IV

EXPERIMENTAL APPARATUS AND DESIGN CRITERIA

A. Fin Tube Construction

The three fin tubes used in this investigation were fabricated from a solid round bar of 65S-T6 aluminum alloy on a No. 2 universal milling machine, utilizing a table driven dividing head to produce the helical fin surfaces. The fin tubes were designated by I, II, and III having leads of 3.24 in., 4.48 in. and 6.48 in. respectively. Other manufacturing techniques were considered for fabricating the fin tubes, such as, welding the helical fin surfaces to a round tube. However, the possibility of a non-uniform weld at the bond line between the fins and the tube could adversely affect the heat transfer characteristic of the fin tubes and complicate the analysis of the problem. Therefore, the additional time spent in machining the tubes was justified.

Prior to the actual milling operation, a 1.750 in. dia. core hole was drilled axially and concentric to the 4.260 in. dia. of the 65S-T6 aluminum section to produce a cavity for the heater rod. Since the linear capacity between centers of the milling machine was 12.0 in., three separate sections each approximately 11.0 in. long by 4.260 in. dia. were machined for each pitch of fin tube. The three sections were assembled in the axial direction after milling by means of a press fit sleeve-socket connection.

To ensure the integrity of the axial alignment, two 0.25 in. dia. by 0.25 in. long steel set screws were tapped radially 180° apart in each of the two sleeve-socket connections, thus eliminating any extraneous distortion caused by thermal expansion in the axial direction. Upon final alignment, the mating surfaces of the fins between adjacent sections were lapped to present a smooth continuous surface to the air flow.

Concentric alignment of the fin tubes inside the annulus was assured by use of eight 4-40 steel set screws tapped radially into the fin tips. For each annulus tested the screws were adjusted to maintain concentric alignment of the fin tube.

B. Annulus

The annular test sections used in this investigation were formed from commercial grade, low carbon, seamless mechanical tubing having a wall thickness of 0.120 in. and a length of 10.0 ft. The annuli were designated by A, B, and C having inside diameters of 4.260 in., 4.500 in., and 5.010 in. respectively.

Four static pressure taps spaced 90° apart were installed on the exterior surface of each annulus at Stations No. 1 and No. 5. In addition, two static pressure taps spaced 180° apart were installed at Station No. 3 for each annulus. The static pressure tap holes were 0.040 in. dia. and care was exercised to remove any burrs on the interior surface of the annulus test section left by the drilling operation.

To facilitate entry of the manually operated air temperature probe and exit of the fin tube surface thermocouple leads, two axial

slots each 4.0 in. long by 0.125 in. wide were milled 180° apart at both Stations No. 2 and No. 4 for each annulus.

The exit of the fin tube surface thermocouple leads at Station No. 1 was accommodated by a 0.500 in. I.D. copper tube soldered over a 0.500 in. dia. hole drilled 24.0 inches in front of Station No. 1. To prevent the edges of the copper tube and annulus from fraying the thermocouple wire insulation, a 0.500 in. O.D. by 0.125 in. thick wall "Tygon" tube sleeve was inserted into the copper tube and a small cork was fitted into the sleeve, thus forming an effective packing gland and eliminating leakage of the coolant air from the annulus.

Heat loss from the annulus to the ambient room was minimized by means of a three-layer lagging. A 0.005 in. thick layer of reflective aluminum foil was first applied to each annulus between Stations No. 1 and No. 5. This was followed by a 1.0 in. thick layer of commercial grade fiberglass pipe insulation, having a thermal conductivity of 0.027 Btu/hr. ft. °F. Finally, another layer of reflective aluminum foil was added to keep the fiberglass particles from contaminating the laboratory.

To prevent the fin tube from moving axially in the direction of air flow, a hold-in clamp was fabricated at the exit end of each annulus. Axial movement was restricted by means of a 0.375 in. dia. by 18.0 in. long aluminum rod held concentric with the fin tube axis by the hold-in clamp. Since the aluminum rod also served as the electrical buss, it was electrically insulated from the hold-in clamp by a nylon insulator bushing.

C. Heater

The prime consideration in selecting a method of heating the fin tube was to obtain the highest heat flux density per unit length. A nuclear energy heating source was immediately eliminated because of the high cost and safety hazards present. On the other hand, heating by condensing steam or circulating hot fluids through the fin tube core was discarded because of the relatively low heat flux available. An electric resistance heater was therefore chosen because of its high heat flux and ease of application to the fin tube core. In addition, electric resistance heating offered both ease of control and precise determination of heat flux generated in the heater. Two methods of electric resistance heating were initially considered for heating the fin tube. These are:

1. Calrod cartridge heater.
2. Radiant heat from a high temperature source.

The calrod heater method was discarded in favor of the second method because of the difficulties involved in producing a precision reamed core hole axially through the fin tube for a length of 33.625 in. A uniform diameter hole is necessary to minimize the extraneous effects of a variable thermal contact area, since the calrod heater transfers its heat in the conduction mode. The radiant heater method completely eliminates the thermal contact area problem by supplying its heat flux to the fin tube in the radiation mode. In addition, the radiant heater method allowed the heater rod to be interchanged with the different fin tubes, thus reducing the need of three separate heating units.

The heater rod was constructed from a 0.75 in. dia. by 42.0 in. long commercial grade silicon carbide electric furnace "Glowbar". The rod was formed by recrystallization of silicon carbide at an elevated temperature. The central section of the rod 34.0 in. long, designated the hot zone, had an electrical resistivity of 0.11 ohm-cm. at 2000°F. Two terminal sections, designated cold ends, each 4.0 in. long was bonded to the hot zone at the time of recrystallization. These terminal ends were impregnated with a powdered metal and have an electrical resistivity of 0.005 ohm-cm at 70°F. A ratio of resistivity of 22:1 between the hot zone and the cold ends assured a minimum of heat generation in the cold ends, thus allowing the use of metal contact terminals for the electrical connection to the power supply leads.

Mounting of the heater rod axially and concentric within the 1.750 in. dia. core hole of the fin tube was achieved by two "Transite" fairing cones (Fig. No. 4). The fairing cones had the dual role of mounting the heater rod and minimizing the abrupt entrance and exit effects of the air flow stream on the fin tube.

Preliminary experiments indicated that a temperature of 800°F existed in the region of transition between the hot zone and the cold ends. To eliminate thermal degradation of the "Transite" exposed to this high temperature, a layer of ceramic refractory serviceable to 3000°F, was bonded over the exposed areas of the "Transite".

To prevent air leakage from the flow stream into the heater rod cavity at the interface between the fairing cones and the fin tube,

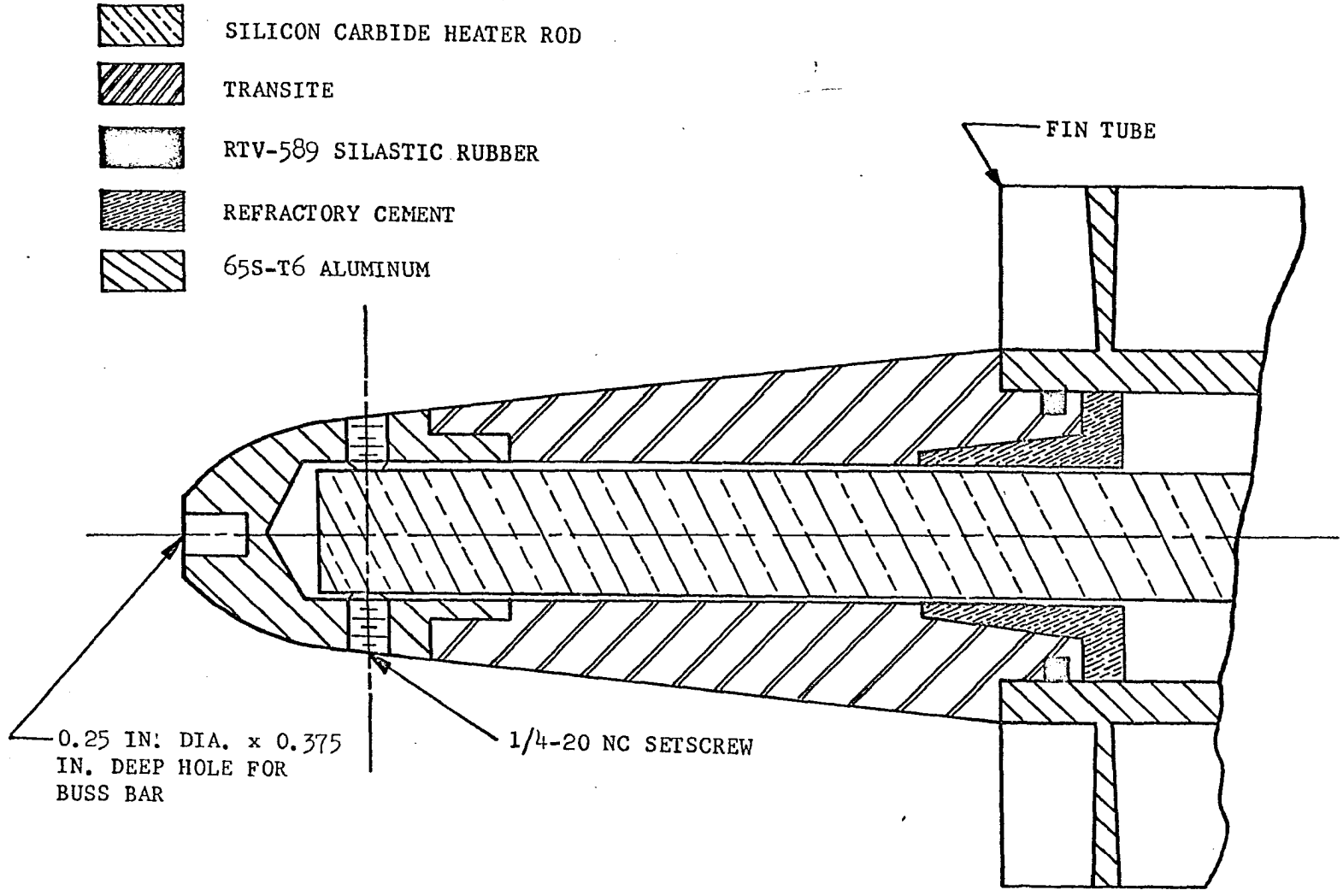

FIGURE NO. 4 CROSS-SECTIONAL VIEW OF FAIRING CONE (not to scale)

a gasket was formed by curing Dow-Corning RTV-589 "Silastic Rubber", serviceable to 600°F, on assembly of the fairing cones and fin tube.

D. Heater Power Supply and Instrumentation

Electric power from a 120 volt, single phase, 60 cycle source was used to heat the heater rod. Fluctuations in the source voltage were minimized by a General Radio Company automatic voltage regulator, Type 1570-ALS15 rated at an output voltage of 120 volts ±0.25% at a 50.0 ampere load (Fig. No. 5).

Temperature versus resistivity characteristics of the silicon carbide heater rod necessitated reduced voltage cold starting to prevent the heater rod from cracking due to transient thermostresses. Therefore, a General Radio Company "Variac", Model W-50 rated at 0-140 volts output at 50.0 amperes load was utilized to bring the heater up to operating temperature and adjust the heating load.

The actual power dissipated in the heater rod was determined by a laboratory grade wattmeter of ±1.0% accuracy. The current coil of the wattmeter was connected to a precision grade current transformer in the "Variac"-heater rod circuit. The current transformer provided a 10:1 ratio of input to output at an accuracy of ±0.25%. The potential coil of the wattmeter was connected directly across the heater rod.

In addition to the wattmeter, a voltmeter and ammeter were also connected into the power circuit. The product of their readings, volts x amps, provided a check on the wattmeter. Since the heater rod offered a pure resistive load to the power supply, a power factor of 1.0 was assumed.

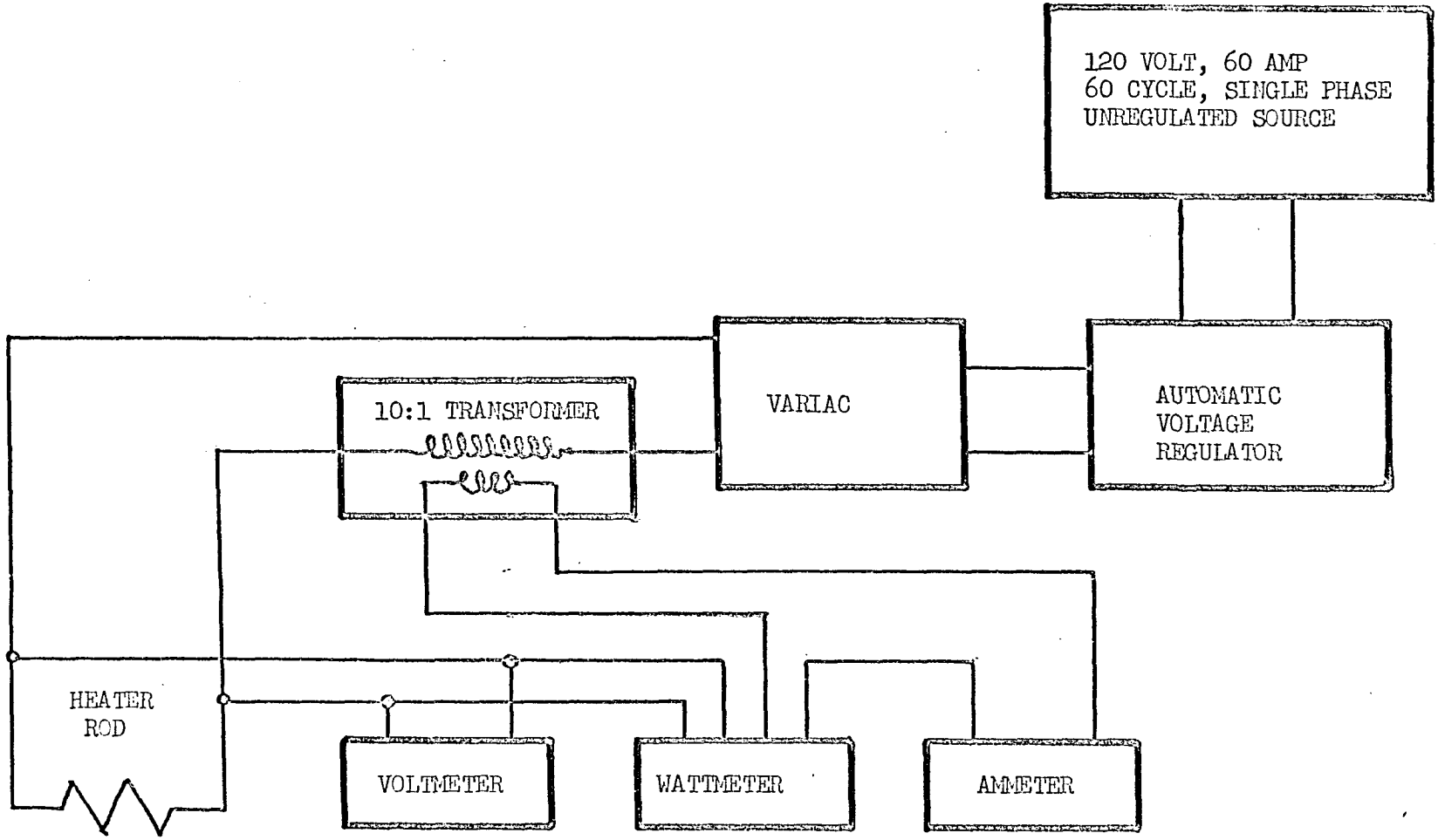

FIGURE NO. 5 SCHEMATIC DIAGRAM OF POWER CIRCUIT

E. Air Supply

Coolant air was supplied to the annular test section from an American Blower Corporation, Type "1V" industrial centrifugal fan driven by a 208 volt, 3-phase, 3 hp induction motor. Modulation of the airflow to the annular test section was achieved by means of a butterfly valve placed on the inlet port of the fan. A short piece of flexible rubber tubing was installed between the exit port of the fan and the inlet section of the air flow measuring stand to dampen any mechanical vibration produced by the fan and motor.

F. Air Flow Measurement

The quantity of air supplied to the annular test section was determined by a flow measuring stand constructed to the specifications of Reference No.20. The velocity pressure of the air stream was obtained from a 0.125 in. O.D. pitot-static tube placed on the axial centerline of a smooth drawn copper tube 3.055 in. I.D. by 12.0 ft. long. A bundle of flow straighteners formed from 0.062 in. wall thickness by 0.500 in. O.D. by 4.0 in. long copper tubing was placed 4.0 ft. ahead of the pitot-static tube to minimize the turbulence induced by the fan. The axial centerline velocity pressure was measured on a Meriam Instrument Company inclined manometer, Model 40HA10, with a range of 0.0 to 6.0 in. water pressure.

Calibration of the pitot-static tube in the axial centerline position was achieved by two ten-point traverses 90° to each other. The ratio of average velocity pressure to the axial centerline

velocity pressure was found to be 0.89 for the range of flow rates used.

In addition, a four point fixed thermocouple probe was placed radially and 1.0 in. behind the pitot-static tube to measure the temperature of the air stream.

G. Pressure Measurement

The static pressure drop along the annular test section was measured by a T.E.M. Instruments, Limited, multitube inclined manometer with an accuracy of ±0.025 in. water pressure. A total pressure profile of the air flow in the radial direction was obtained at Stations No. 2 and No. 4 by a 0.062 in. dia. Kiel probe mounted on a screw actuated traversing mechanism. The accuracy of the screw allowed the probe to be positioned to ±0.005 in.

Barometric pressure was obtained from a laboratory grade barometer accurate to ±0.01 in. mercury.

H. Temperature Measurement

Fin tube surface temperatures were determined by 30 gauge teflon insulated duplex copper-constantan thermocouples. Preliminary experiments indicated a reliable bond between the aluminum surface and the thermocouple measuring junction could not be attained by capacitor-discharge spotwelding. Therefore, the following procedure was developed to attach the thermocouples to the fin tube surface.

A 0.020 in. dia. by 0.050 in. deep hole was drilled at each thermocouple location with a high speed dental drill. The thermocouple measuring junction was formed by inserting the two 0.010 in. dia.

wires side by side into the drilled hole. The metal adjacent to the hole was peened into the hole and around the wires, thus forming a sound mechanical and thermal bond. The thermocouple wires were bent axially in the direction of flow along the fin tube surface for at least 1.0 in. and a drop of "Epoxylite-813" adhesive serviceable to 500°F, was applied to the wires to prevent the air stream drag from pulling them loose from the thermocouple junction.

The fin tube surface thermocouple leads at Station No. 1 were brought out of the annular test section through the 0.500 in. dia. copper tube described in Part B of this chapter. At Stations No. 2 and No. 4 the fin tube surface thermocouple leads were brought out through the 4.0 in. long axial slots also described in Part B. Air leakage from the annular test section through the slots was eliminated by applying several layers of a heating duct adhesive tape, serviceable to 350°F, over the slots and thermocouple leads.

Air inlet temperature to the annular test section at Station No. 1 was determined by four thermocouples located in the air flow measuring stand described in Part F of this chapter. Exit air temperature from the annular test section at Station No. 5 was determined by eight 30 gauge copper-constantan thermocouples placed radially through the annulus wall.

The air temperatures at Stations No. 2 and No. 4 were obtained from a shielded total temperature type probe mounted on the same traversing mechanism as described in Part G of this chapter. The probe was constructed from 0.125 O.D. by 0.020 in. wall thickness 304 stainless steel tubing. A 0.125 in. dia. shield was employed

around the thermocouple measuring junction to minimize errors induced by thermal radiation from the fin tube surface.

Temperature distribution through the lagging on the annular test section was obtained from thermocouples placed on the interior and exterior radii of fiberglass pipe insulation at Stations No. 1, No. 3, and No. 5. The thermocouple wire was wound circumferentially about the insulation to minimize error induced by thermal conduction along the wires.

All thermocouple wire used in this investigation was calibrated and certified by the manufacturer to be within a tolerance of ±0.75°F over a range of -75° to 400°F. E.m.f.'s generated by the fin tube surface thermocouples were measured and recorded on a Weston Instrument Company multi-point stripchart recorder, Model 6702, range 0° to 510°F with an accuracy of ±0.2% full scale. Air temperatures at Stations No. 2 and No. 4 were measured on a Leeds and Northrup potentiometer, Model 8693, range -100° to 400°F with an accuracy of ±0.2%. Prior to each test run, both potentiometers were calibrated to within ±0.010 millivolts by comparison to a Cambridge Instruments Company, Limited, microstep precision potentiometer, Model 44248 with an accuracy of ±0.1 microvolt.

Wet and dry bulb temperatures for the relative humidity determination were measured by a laboratory grade sling psychrometer with an accuracy of ±0.5°F.

CHAPTER V

EXPERIMENTAL RESULTS AND DISCUSSION

The object of this investigation was to determine the effects of pitch and fin tip clearance on the heat transfer and pressure drop characteristics of the fin tube-annulus arrangement. All other geometric parameters remained the same throughout the experiment. The variation in pitch for the three fin tubes tested was as follows:

Fin tube I: pitch = 0.650 in.

Fin tube II: pitch = 0.955 in.

Fin tube III: pitch = 1.400 in.

The annulus clearance could be varied by interchanging the fin tubes with three different outer tubes and these clearances were designated by the following notation:

Annulus A: Clearance = 0.0 in.

Annulus B: Clearance = 0.140 in.

Annulus C: Clearance = 0.375 in.

The heat flux input to the fin tube from the silicon carbide heater rod was maintained at a value of 5.0 kilowatts for all test runs and the air flow rate was varied to give a range of Reynolds Numbers from 9000 to 43,000.

A. Test Procedure

For each fin tube-annulus combination tested the following procedure was observed. The selected fin tube was fitted in the

annulus and was positioned concentrically to within a tolerance of ± 0.010 inch. In addition the fin tube was positioned axially between the static pressure taps at Station No. 1 and No. 5 to within a tolerance of ± 0.015 inch. The fan was started and the flow control valve on the inlet of the fan was positioned to give maximum air delivery. The heater power supply was then activated and the heat load adjusted to 5.0 kilowatts. The air flow rate was decreased until a maximum temperature of $400^{\circ}F$ was recorded at the fin tube surface and steady state conditions prevailed. The air flow rate was adjusted between the minimum delivery and the maximum delivery to give five Reynolds Numbers for each fin tube-annulus tested. For each steady state flow rate, the following data was collected:

1. Barometric pressureand relative humidity.
2. Inlet air temperature and centerline velocity pressure at the flow measuring stand.
3. Air temperature at Stations No. 1, 2, 4, and 5 designated by: T_{b1} , T_{b2} , T_{b4}, T_{b5} respectively.
4. Fin tube surface temperatures at the root, mid-point, and tip of the fins at Stations No. 1, 2, 4 and 5; typically designated by the following notation:

   T_{SR1} = Surface temperature of fin root at Station No. 1

   T_{SM1} = Surface temperature of fin mid-point at Station No. 1

   T_{ST1} = Surface temperature of fin tip at Station No. 1

etc.

.

.

etc.

.

.

T_{ST5} = Surface temperature of fin tip at Station No. 5

5. Temperature at inner and outer surface of the annulus insulation at Stations No. 1, 3, and 5; typically designated:

T_{I1} = Inner surface temperature of insulation at Station No. 1

T_{01} = Outer surface temperature of insulation at Station No. 1

.

.

etc.

.

.

T_{05} = Outer surface temperature of insulation at Station No. 5

6. Static pressure at Stations No. 1, 3, and 5.

7. Electric power input for heat flux determination.

B. Data Reduction

To aid in reducing the large number of data generated by this investigation, two Fortran II computer programs were compiled for an IBM 1620 Mk II digital computer. Program Number 1 took the appropriate input data and computed numerical values for the Reynolds Number, Prandtl Number, Nusselt Number, and the Fanning friction factor. Program Number 2 provided numerical values for the fin efficiencies. Using a standard program for the statistical method of multi-linear regression, the data was correlated according to Equation (3-18) and the constant (a_1) and the exponents b_1, b_2, and b_3 determined.

C. Heat Transfer

The variation of heat transfer with Reynolds Number for the variables of fin pitch and annular clearance is shown in Figures No. 6 and No. 8. The correlations of these geometric variables are presented in Figures No. 7 and No. 9. A typical temperature distribution of the fin tube surface and air in the axial direction is shown in Figure No. 10. Fig. No. 11 shows the variation of fin efficiency with the parameter $\left[\frac{Z^2 h_m}{W k}\right]$.

The determination of the fin efficiency (ϕ) was one of the areas that could be readily investigated, as the relatively large fin pitch allowed thermocouples to be directly attached to the fin tube surface without greatly disrupting the flow pattern. Another factor that necessitated this measurement was the peculiar fin profile left by the manufacturing process, the fin profile being thicker at the fin tip than at the root. This type of profile is uncommon in heat transfer applications as the usual practice is to utilize a fin of minimum weight, i.e., the profile is thicker at the fin root than at the fin tip. In addition analytical predictions for this inverted profile were unavailable.

The fin efficiency was determined from Equation (3-6) where the average fin surface temperature (T_{SA}) was determined from the measured temperature gradient in the fins at Stations Nos. 1, 2, 4 and 5. Since the temperature gradient varied slightly at each station, the fin efficiency also varied in the axial direction. An area weighted average of (ϕ) was calculated for each test run and the results are presented in Table No. 5.

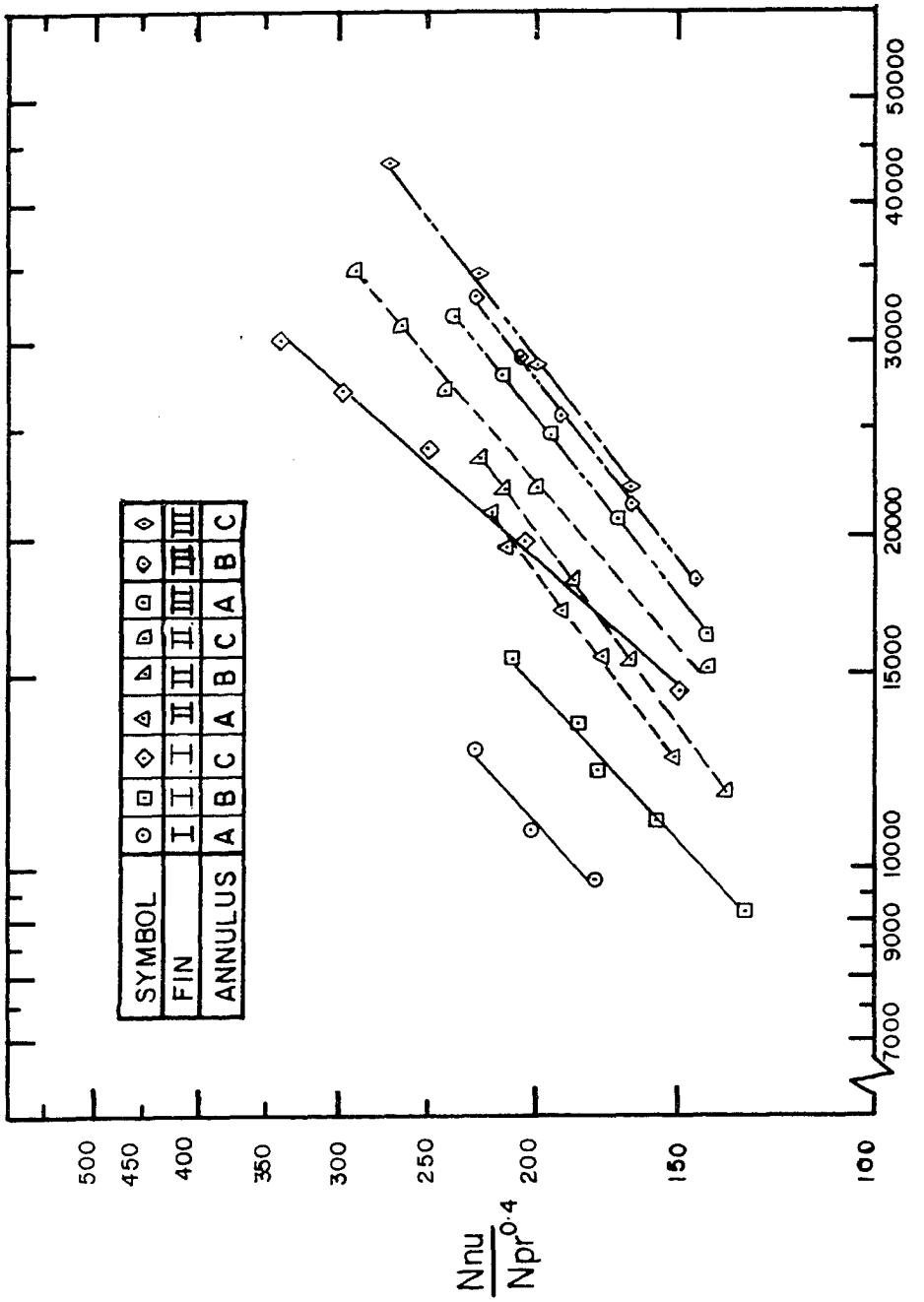

FIGURE NO. 6 DIMENSIONLESS HEAT TRANSFER TERM BASED ON ΔT_{lm} V.S. REYNOLDS NO.

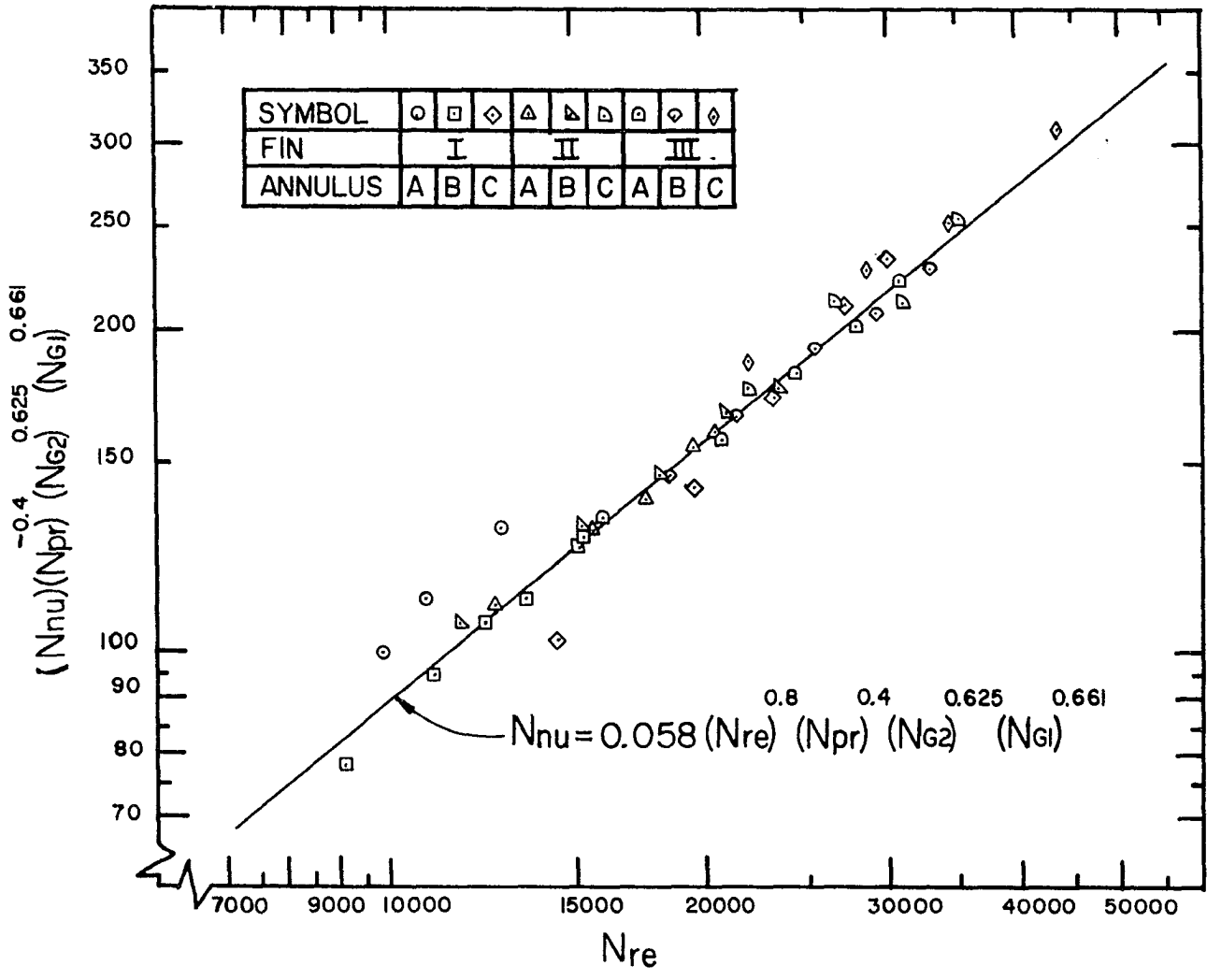

FIGURE NO. 7 CORRELATION OF DIMENSIONLESS VARIABLES OF THE HEAT TRANSFER TERM BASED ON ΔTlm V.S. REYNOLDS NO.

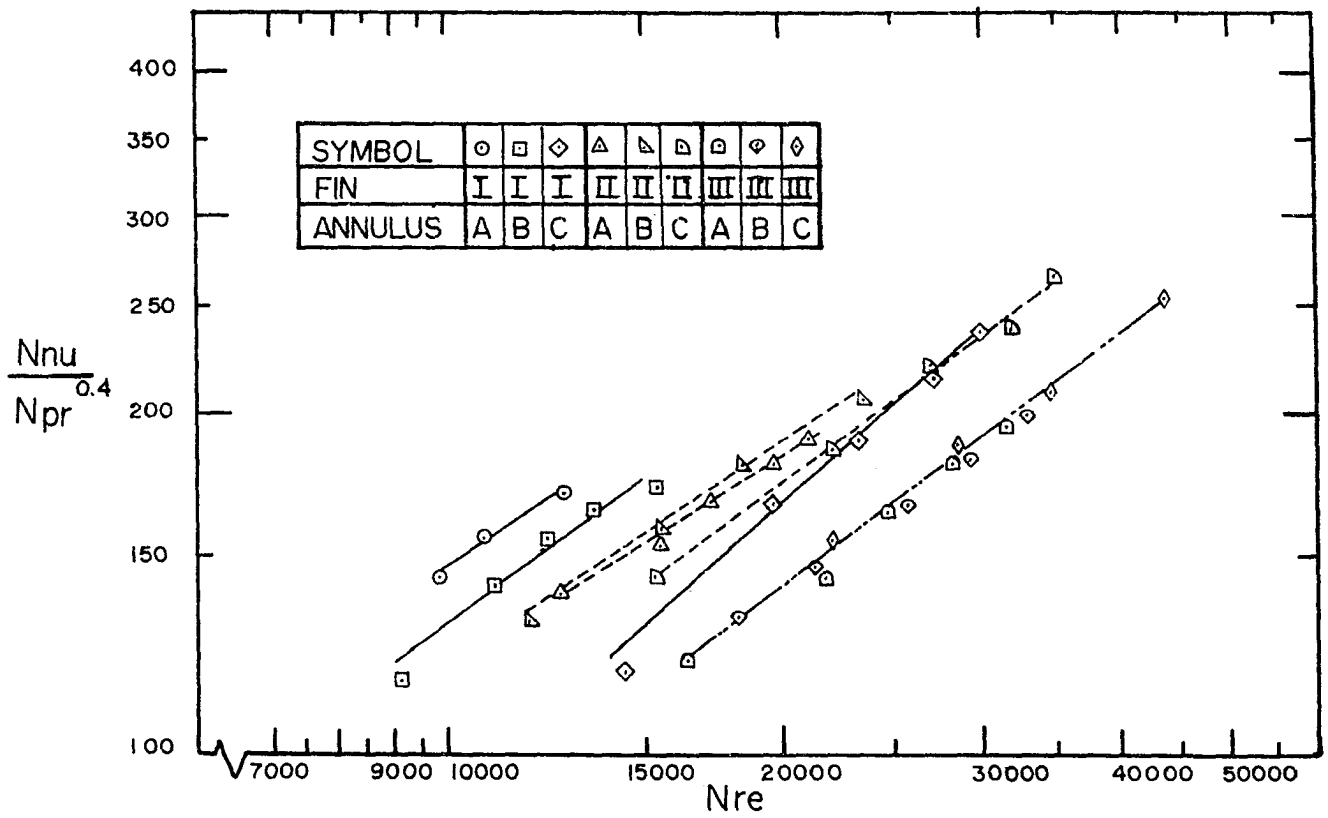

FIGURE NO. 8 DIMENSIONLESS HEAT TRANSFER TERM V.S. REYNOLDS NUMBER BASED ON SEGMENTED $\Delta T'm$

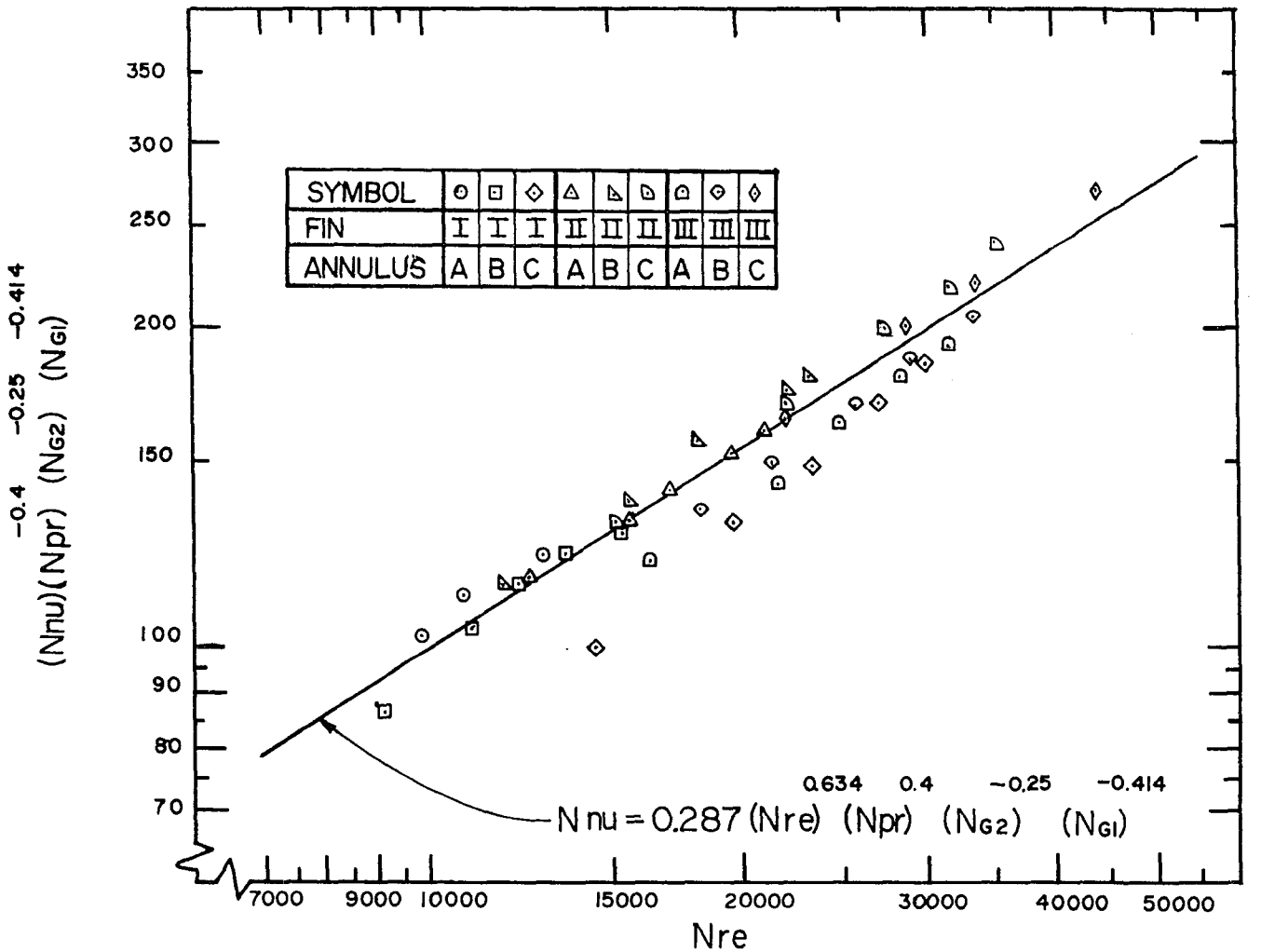

FIGURE NO. 9 CORRELATION OF DIMENSIONLESS HEAT TRANSFER TERM BASED ON SEGMENTED $\Delta T\bar{m}$ V.S. REYNOLDS NO.

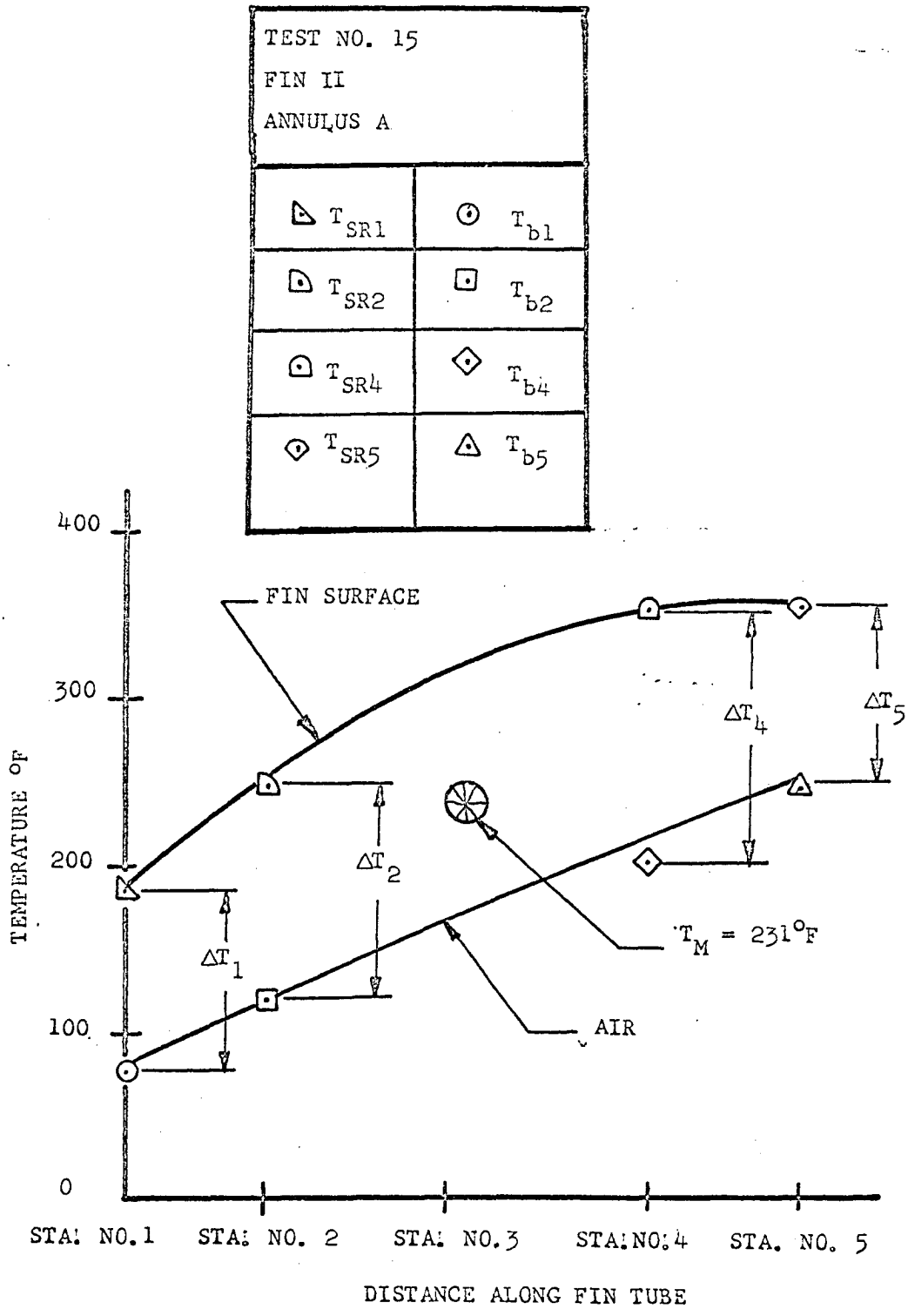

FIG. NO. 10 TEMPERATURE DISTRIBUTION OF FIN TUBE SURFACE AND AIR ALONG FIN TUBE AXIS

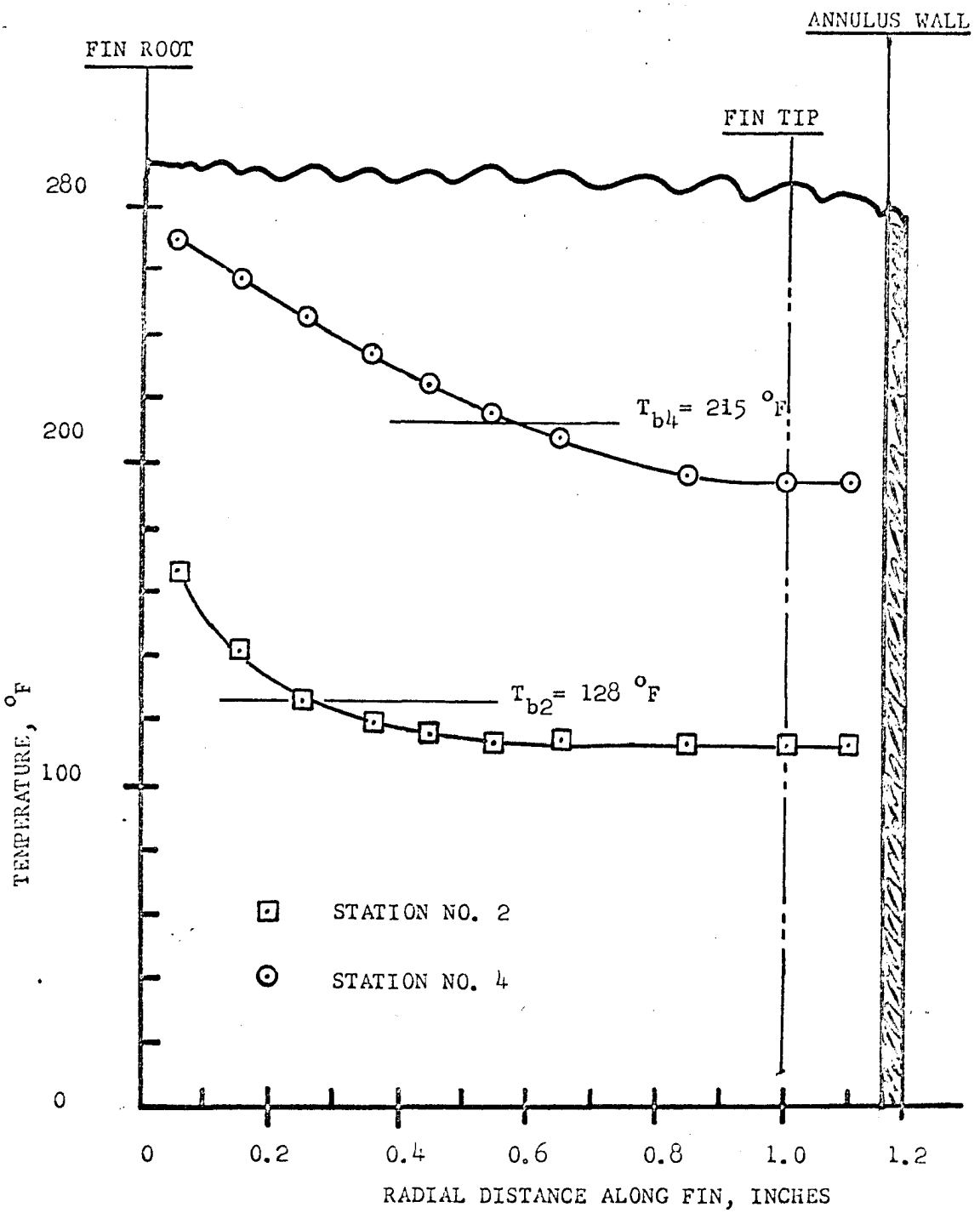

FIG. NO. 10A RADIAL TEMPERATURE GRADIENT OF AIR AT STATION NO. 2 AND STATION NO. 4 FOR TEST NO. 15, FIN TUBE II ANNULUS A

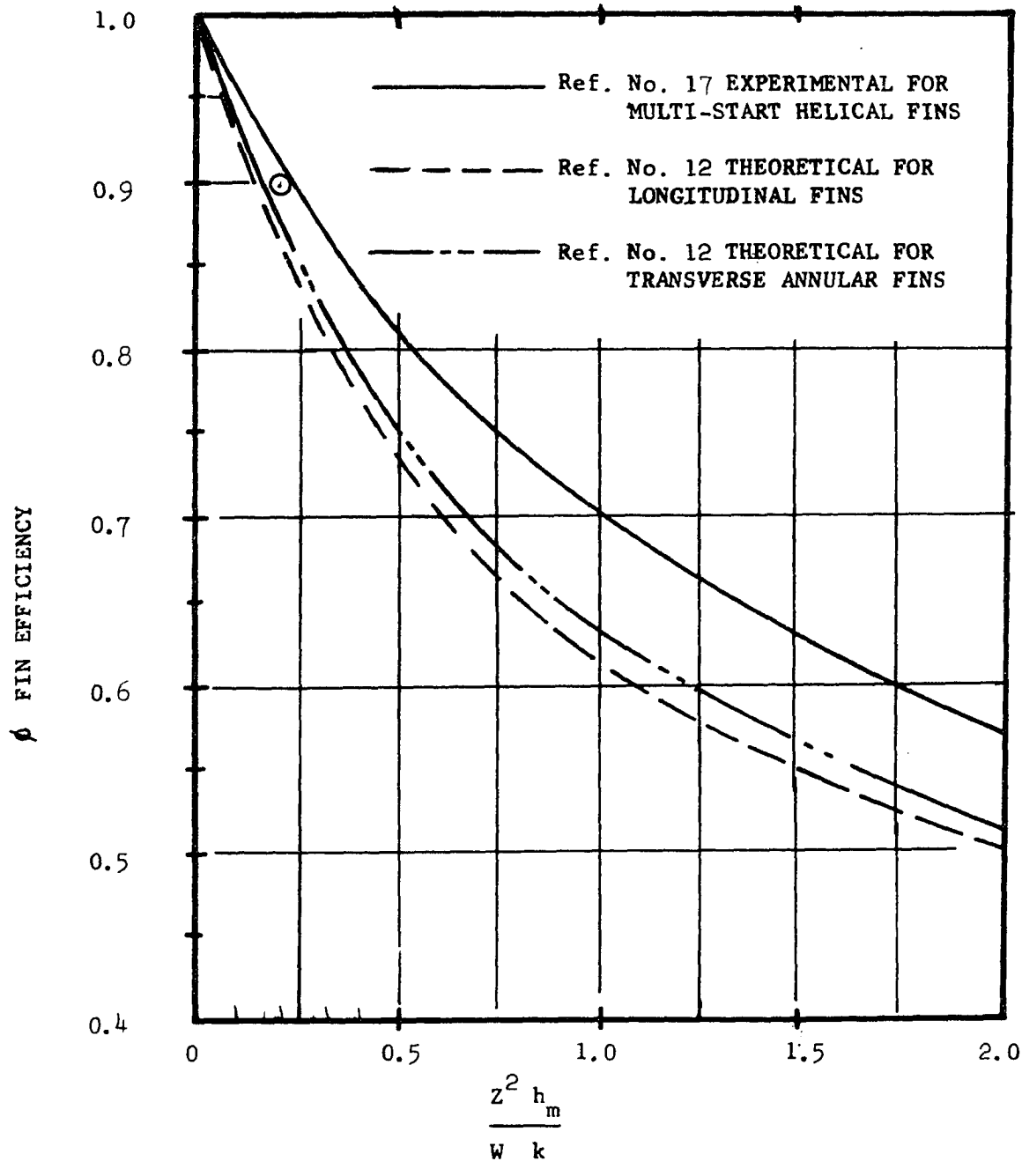

ϕ = Fin efficiency

Z = Fin height

h_m = Average heat transfer coefficient

W = 1/2 average fin thickness

FIG. NO. 11 EXPERIMENTAL AND ANALYTICAL FIN EFFICIENCIES FOR STRAIGHT, HELICAL AND TRANSVERSE FINS

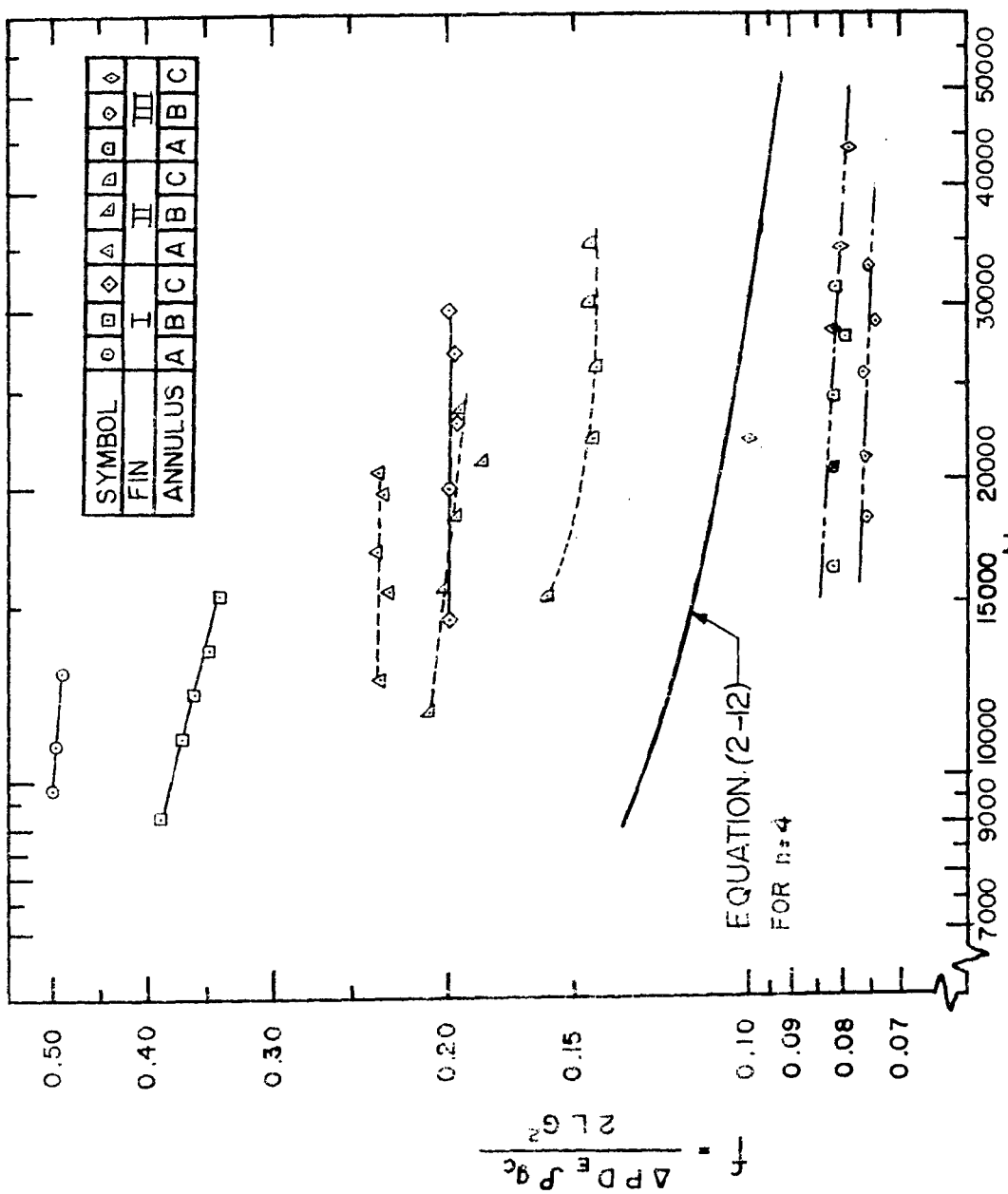

FIGURE NO.12 FRICTION FACTOR VS REYNOLDS NUMBER

A comparison of the experimental fin efficiencies obtained in this investigation with that of Gardner's[12] analytical solution and Cunningham and Slack's[17] experimental work is shown in Figure No. 11. Since the fin profile tapered slightly, an average fin thickness was used for comparison to both references. For this investigation the fin efficiency (ϕ) was found to range from 0.870 to 0.934. Hence, for the sake of comparison a data point where the heat transfer coefficient (h_m) = 20.0 Btu/hr ft^2 $^\circ$F was evaluated in Figure No. 11. As might be expected the resulting value of (ϕ) lies between that of helical fins and transverse annular fins.

The average heat transfer coefficient (h_m) between Station Nos. 1 and No. 5, based on Equation (3-10) was used in calculating the Nusselt Number in Fig. No. 6 and No. 7. Since there was an axial temperature gradient in both the air and on the fin tube surface, the physical properties of the air were evaluated at (T_M), the mean temperature difference between the air and the fin tube surface. The temperature (T_M) shown in Fig. No. 10 was obtained from the relation:

$$T_M = \frac{\overline{T}_{SR} + \overline{T}_b}{2} \qquad \text{Eq. (5-1)}$$

where $\overline{T}_{SR}$ = Average fin tube surface temperature obtained from graphical integration between Station No. 1 and No. 5.

$\overline{T}_b$ = Average bulk air temperature obtained from graphical integration between Sta. No. 1 and No. 5.

The bulk air temperatures T_{b1}, T_{b2}, T_{b4}, and T_{b5} were obtained from the radial temperature gradient in the air at each station. The radial temperature gradient of the air for any one station was

determined by a ten point traverse utilizing the probe described in Part H of Chapter IV. Since the velocity at each traverse point was unknown, the bulk air temperatures were determined by graphical integration as shown in Figure No. 10A.

Relative humidity data was obtained for each test run. However, no attempt was made at controlling this variable as its influence on the physical properties of air was less than 1.5% for the range of this investigation.

Figure No. 6 shows the effects of the geometric variables of pitch (P) and radial clearance (R_c). As (R_c) is increased, the heat transfer drops off significantly. This can be attributed to the regime of air flow within the annular test section. As (R_c) is increased, the air flow stream tends to leave the heated channels formed by the fins and flow axially in the annular area adjacent to the outer wall. Since the air flow tends to follow the path of least resistance, i.e., towards the cooler annulus wall, the temperature difference between the heated fin tube surface and the air is increased, thus resulting in a decrease in heat transfer coefficient. Also, as the fin tube pitch is increased, the free flow area (A_n) is increased and the turbulent mixing induced by the helical surface is decreased resulting in a decrease in the heat transfer coefficient (h_m).

Figure No. 7 shows the correlation of the geometric variables of pitch and radial clearance obtained from the procedure outlined in Equations (3-17) and (3-18). The correlation coefficient, i.e., the measure of "goodness" of fit was found to be 0.9633, where 1.0 is perfection. The correlation equation was found to be:

$$N_{Nu} = 0.058\ (N_{Re})^{0.8}\ (N_{Pr})^{0.4}\ (N_{G2})^{0.625}\ (N_{G1})^{0.661}$$

Eq. (5-2)

A check on the average of the heat transfer coefficients between Stations No. 1 and No. 2; Stations No. 2 and No. 4; and Stations No. 4 and No. 5 indicated that they were 10 to 20% less than the heat transfer coefficient (h_m) obtained between Stations No. 1 and No. 5. Referring to Fig. No. 10, it can be seen that the temperature difference between the air and the fin tube surface is greater at Station No. 3 than at either Station No. 1 or Station No. 5. Therefore Equation (3-9) will give a smaller value for (ΔT). To obtain a more realistic value of the temperature difference, an area weighted segmented value was calculated between each station:

$$\Delta T'_{lm\ 1-5} = \frac{\Delta T_{lm\ 1-2} A_1 + \Delta T_{lm\ 2-4} A_2 + \Delta T_{lm\ 4-5} A_3}{A_1 + A_2 + A_3} \qquad \text{Eq. (5-3)}$$

$\Delta T'_{lm\ 1-5}$ = Segmented $(LMTD)'$ between Stations No. 1 and No. 5

$\Delta T_{lm\ 1-2}$ = LMTD between Stations No. 1 and No. 2

$\Delta T_{lm\ 2-4}$ = LMTD between Stations No. 2 and No. 4

$\Delta T_{lm\ 4-5}$ = LMTD between Station No. 4 and No. 5

A_1 = Effective heat transfer area between Stations No. 1 and No. 2

A_2 = Effective heat transfer area between Stations No. 2 and No. 4

A_3 = Effective heat transfer area between Stations No. 4 and No. 5

The heat transfer coefficients based on this new ($\Delta T'_{lm}$) are shown in Fig. No. 8. The Nusselt Numbers in this case are approximately 20% lower than those for the corresponding curves in

Fig. No. 6. Figure No. 9 shows the correlation of the heat transfer coefficients in terms of the pitch and radial clearance. The correlation coefficient was 0.92157 and the correlating equation was found to be:

$$N'_{Nu} = 0.286 (N_{Re})^{0.634} (N_{Pr})^{0.4} (N_{G2})^{-0.250} (N_{G1})^{-0.414}$$

Eq. (5-4)

The unusual temperature distribution curves, of which that shown in Fig. No. 10 is typical, and necessitated the two correlations, can probably be attributed mainly to end effects such as heat conduction into the heater rod fairing cones (see Fig. No. 4), and a sudden expansion in the air flow at Station No. 5. The justification for presenting the two correlations lies in the use made of them. In most applications the designer is interested in the overall heat transfer and inlet and outlet temperatures only, and in this circumstance correlating Equation (5-2) can be used. However, if a knowledge of the variation in temperature along the fin tube is available, then Equation (5-4) is recommended.

D. Friction Factor

The variation of the Fanning friction factor (f) with the Reynolds Number is shown in Figure No. 12. Calculations were made to determine the effect of the term $\frac{T_5 - T_1}{\bar{T}}$ from Equation (3-35) on the friction factor. The results showed that its contribution was less than 2% for the range of temperatures encountered, and consequently the Fanning friction factor with its density term (ρ) evaluated at (T_M) was used to be consistent with other investigations.

Since the purpose of the helically finned surfaces was to promote turbulent mixing of the coolant air within the annular test section the relatively high friction factors, due to the small radial clearances and the short helical lead coupled with the wide fin spacing, were anticipated.

It can be seen that the friction factor was fairly independent of Reynolds Number over the range $10000 < N_{Re} < 43000$ tested. Larger and smaller Reynolds Numbers were impossible to obtain due to the limitations of the air supply, and the permissible upper temperature limit of the aluminum fin.

The effect of radial clearance on the friction factor is quite pronounced, especially for fin tube I. As the radial clearance is increased this friction factor decreases appreciably. This can be attributed to the decrease in rotation induced by the helical surfaces as more air flows in the annular area formed by the radial clearance. Similarly, the effect of pitch on the friction factor is related to the rotation of the air stream. As the pitch is increased, the rotation

decreases and thus the fin tube surface area in contact with the air also decreases resulting in less surface drag.

A comparison between Equation (2-12) based on straight longitudinal fins described in Chapter II under Reference No. 13 is shown. The values of (f) for fin tubes I and II are high as might be expected since the rotation imparted to the air from the helical surface contributes significantly to the drag. However, fin tube III shows a smaller value of (f) over the same range of Reynolds Number. This can be possibly attributed to the effects of higher pressures on the physical properties of the fluid since the data for Equation (2-12) was collected for air and CO_2 at 100 lbf per sq. inch. As mentioned in Chapter III under part B Friction Factor, the effects of pressure on the friction factor were assumed to be negligible for this investigation.

E. Error Analysis

Preliminary experiments on the bonding technique used to fasten the thermocouples to the fin tube surface showed that the circumferential variation in temperature at any station was within $3^{\circ}F$. The average value was used in reporting the fin tubes surface temperatures. Since the bonding technique provided an excellent thermal contact to the fin tube surface, no appreciable conduction error was detected. The results of A- test to determine the effects of the 60 cycle A.C. power line on the thermocouple E.M.F.'s showed no discernable effects on the fin surface thermocouples housed in the annulus.

The static pressure along the length of the fin tube was determined from an inclined water filled monometer set at 30°. For some test runs a fluctuation in the static pressure was observed necessitating an average reading. The combined error in the pressure determination was less than 5%.

Since the air flow rate was determined ahead of the annular test section the possibility of error induced by leakage was minimized by carefully sealing all joints and probing slots, with an adhesive tape. The total combined error due to leakage from the annular test section and the calibration of the flow measuring stand was within $\pm 3.0\%$.

Since the heater rod offered a pure resistive load to the power supply, the electrical energy input was within the $\pm 1.0\%$ accuracy of the wattmeter. Heat lost to the room from the

annular test section was determined by temperature measurements made on the annulus fiberglass insulation. Under the most severe case, i.e., when the fin tips rested on the annulus wall, e.g., fin tube I and annulus A, only 0.35% of the 5.0 kilowatts supplied to the heater was lost.

CHAPTER VI

CONCLUSIONS

The effects of fin spacing (Pitch) and radial clearance (R_c) between the fin tips and outer annulus wall on heat transfer and pressure drop for four start helical fin tubes in steady turbulent annular flow have been presented. On the basis of these results the following conclusions are made:

1A. The heat transfer data can be correlated in terms of the conventional N_{Nu}, N_{Pr}, N_{Re}, and two additional geometric variables N_{G1}, N_{G2} which allow for the variation of Pitch and (R_c).

1B. Equation (5-2), containing the variables mentioned above, correlates the data when a ΔT_{lm}, based on end temperature differences only, is used.

1C. Equation (5-4) correlates the data when the segmented $\Delta T'_{lm}$ is used.

1D. As the pitch increases, for a constant (R_c), the heat transfer coefficient decreases.

1E. As the (R_c) increases for a constant pitch, the heat transfer coefficient decreases.

2A. The friction factor data can be expressed using the Fanning friction factor (f), and for any one fin tube-annulus arrangement are relatively independent of the Reynolds Number.

2B. As the pitch increases, for constant (R_c), the (f) decreases, which is consistent with conclusion 1A.

2C. As the (R_c) increases for constant pitch, the (f) decreases, which is consistent with conclusion (1C.)

3. The fin efficiency (ϕ) of the irregular fin profile used in this investigation agrees substantially with the results of other investigators over the range covered.

REFERENCES

1. Reynolds, O., Proc. Manchester Lit. Phil. Soc. 14:7, (1874).

2. Prandtl, L., Physik Z., 11, (1910).

3. Dittus, F. W., and L. M. K. Boelter, Univ. Calif. (Berkley) Publs. Engr., (1930).

4. Colborne, A. P., "A Method of Correlating Forced Convection Heat Transfer Data and a Comparison with Fluid Friction", TRANS. AIChE., 29, (1933).

5. Wiegand, J. H., "Discussion of Paper by McMillian and Larsen", TRANS. AIChE., 41, (1942).

6. Monrad, C. C., and J. F. Pelton, TRANS. AIChE., 38, (1942).

7. Miller, P., J. J. Byrnes, and D. M. Benforado, J. AIChE, 1, (1955).

8. Gunter, A. Y., and W. A. Shaw, "Heat Transfer, Pressure Drop and Fouling Rates of Liquids for Continuous and Non-continuous Longitudinal Fins", TRANS. ASME, 64, (1942).

9. deLorenzo, B., and E. D. Anderson, "Heat Transfer, Pressure Drop of Liquids in Double Pipe Fin Tube Exchangers", TRANS. ASME., 67, (1945).

10. Knudsen, J. G., and D. L. Katz, "Heat Transfer and Pressure Drop in Annuli", Chem. Engr. Prog., 46, (1950).

11. Chant, R. E., "Convective Heat Transfer from a Helical Fin Tube in Longitudinal Flow", Engr. Institute of Canada, General Meeting Paper No. 63, (1962).

12. Gardner, K. A., "Efficiency of Extended Surfaces", Trans. ASME, 67, (1945).

13. Fortescue, P., and W. B. Hall, "Heat Transfer Experiments on the Fuel Elements", J. Brit. Nucl. Energy Conf., Session 2, (1957).

14. Knudsen, J. G., and D. L. Katz, "Fluid Dynamics and Heat Transfer", McGraw-Hill Co., (1958).

15. Braun, F. W., Jr., and J. G. Knudsen, "Pressure Drop in Annuli Containing Traverse Fin Tubes", Chem. Engr. Prog., 48, (1952).

16. Nikuradse, J., VDI-Forschungsheft, 361, (1933).

17. Cunningham, C., and M. R. Slack, "Heat Transfer and Pressure Drop Performance of Spiral Polyzonal Heat Transfer Surfaces for Gas-Cooled Reactors", Symposium on the Use of Secondary Surfaces for Heat Transfer with Clean Gases, Inst. Mech. Engrs., (1961).

18. Langhaar, H. L., "Dimensional Analysis and Theory of Models", John Wiley and Sons, New York, (1951).

19. Neville, A. M. and J. B. Kennedy, "Basic Statistical Methods for Engineers and Scientists", International Textbook Co., (1964).

20. Air Moving and Conditioning Association, "Standards, Definitions, Terms, and Test Codes for Centrifugal, Axial and Propeller Fans", Bulletin No. 10, Second Edition, A.M.C.A. , 2159 Guardian Bldg., Detroit 35, Michigan.

21. The Carborundum Company, "Glowbar Silicon Carbide Electric Heating Elements, Physical and Electrical Characteristics", Technical Bulletin H, (1958).

22. McAdams, W.H., "Heat Transmission", McGraw-Hill Book Company, New York, (1954).

23. Hsu, T.H., "Engineering Heat Transfer", D. Van Nostrand Co., Princeton, New Jersey, (1963).

24. Kern, D.Q., "Process Heat Transfer", McGraw-Hill Book Co., New York, (1950).

25. Chapman, A.J., "Heat Transfer", The McMillan Company, New York, (1960).

26. Streeter, V.L., "Fluid Mechanics", McGraw-Hill Book Co., New York, (1958).

27. Bureau of Ordnance, Department of Navy, "Handbook of Supersonic Aerodynamics, Vol. 5", (1953).

28. Kays, W.M. and A.L. London, "Compact Heat Exchangers", McGraw-Hill Book Company, New York, (1958).

29 Hall, W.B., "Reactor Heat Transfer", Nuclear Engineering Monographs, Temple Press, London, (1958).

APPENDICES

FIGURES

TABLES

SAMPLE CALCULATIONS

PHOTOGRAPHS

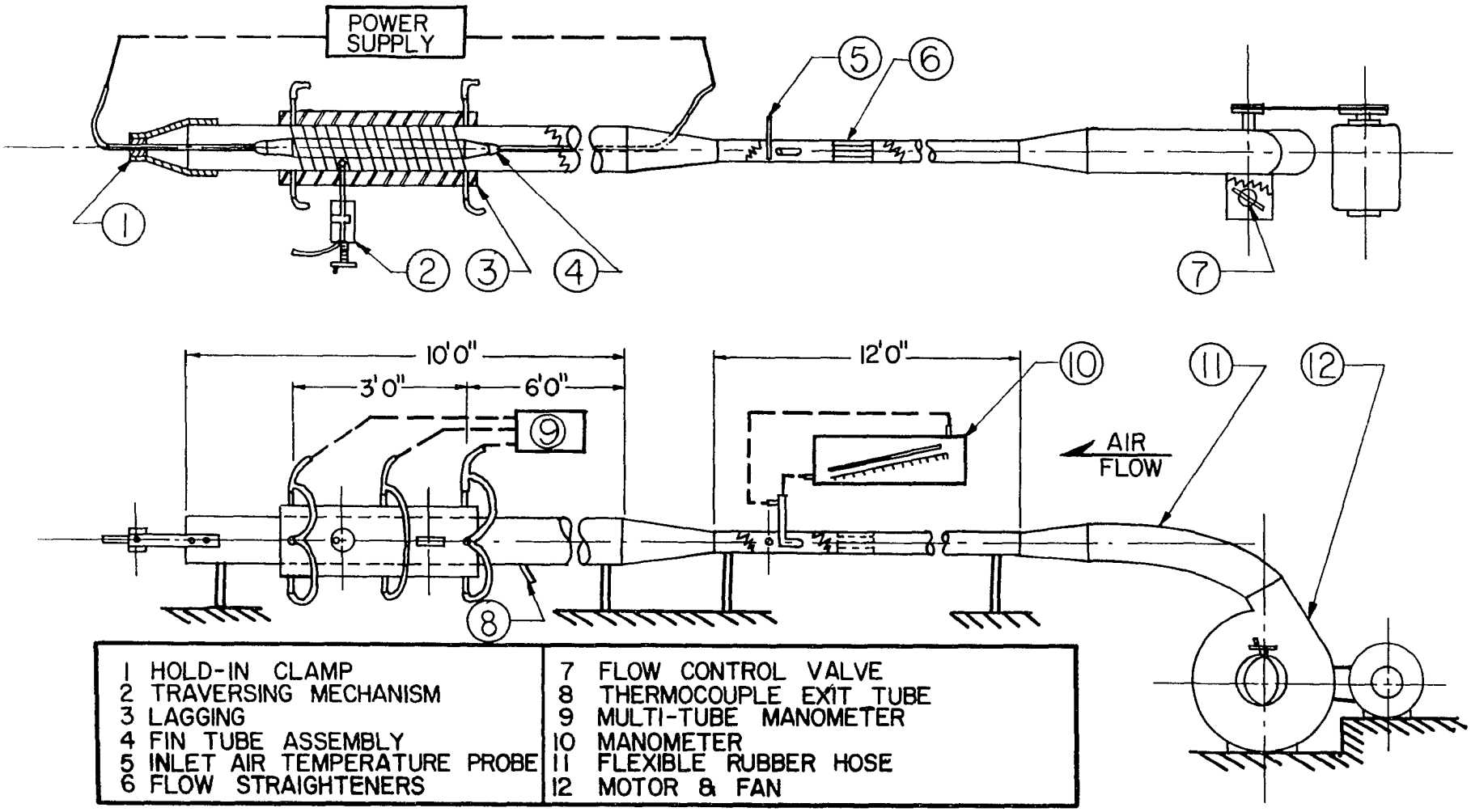

FIGURE NO. 13 SCHEMATIC DIAGRAM OF EQUIPMENT (not to scale)

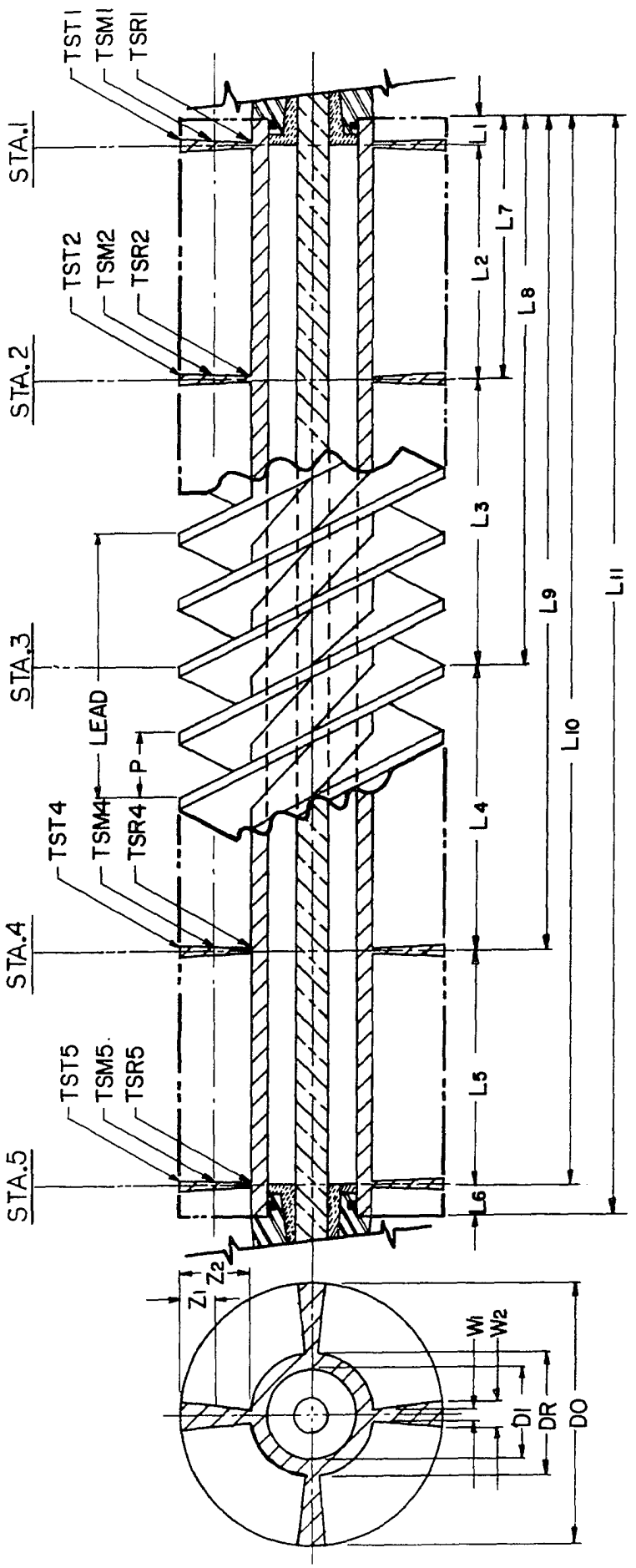

DIMENSIONS COMMON TO ALL FIN TUBES, INCHES												FIN TUBE	LEAD	P	L2	L3-4	L5	L7
DO	DR	DI	W1	W2	Z1	Z2	L1	L6	L8	L10	L11	I	3·24	0·650	10·0	7·31	6·50	10·75
4·230	2·230	1·75	0·12	0·16	0·50	1·00	0·75	0·75	16·81	32·875	33·625	II	4·46	0·955	6·50	9·56	6·50	7·25
												III	6·48	1·400	6·50	10·2	6·00	7·25

FIGURE NO.14 DETAIL DIAGRAM OF FIN TUBES (not to scale)

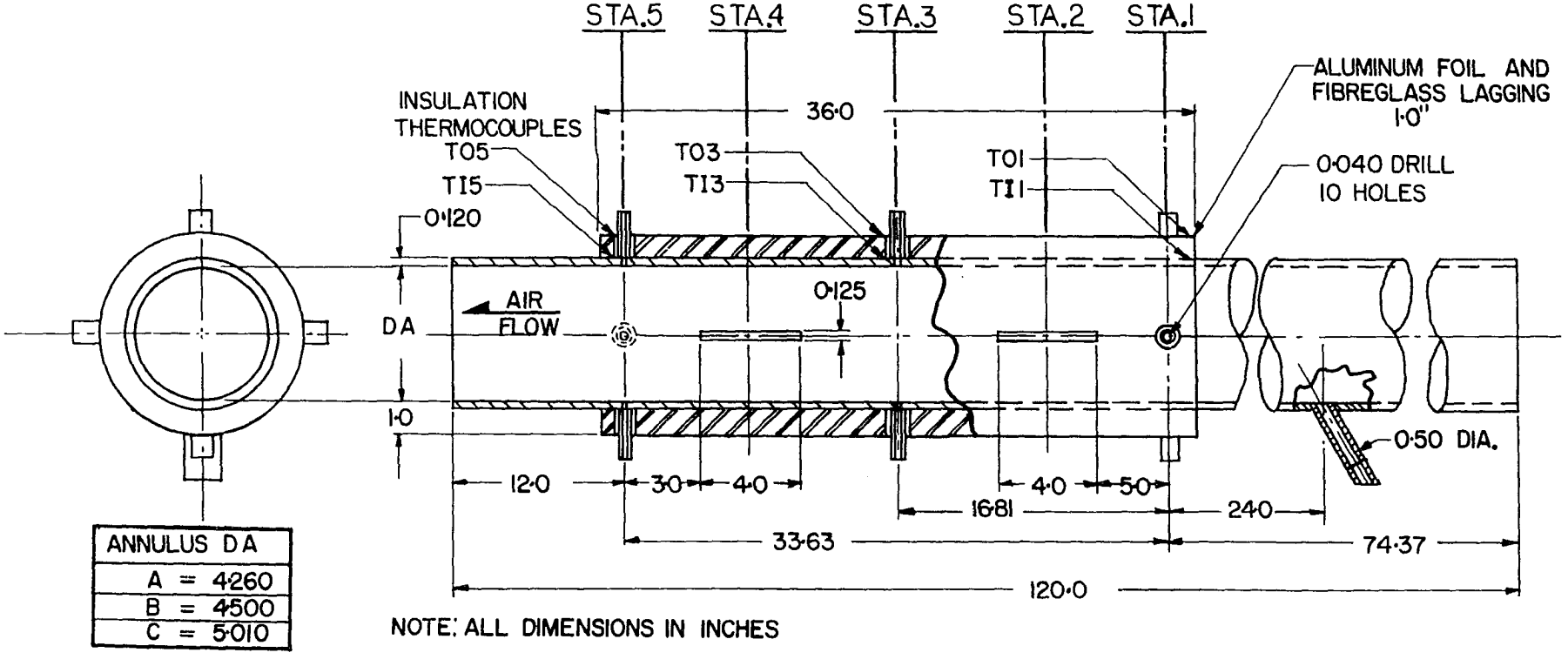

FIGURE NO. 15 DETAIL DIAGRAM OF ANNULI (not to scale)

TABLE NUMBER 1

RELATIVE HUMIDITY, BAROMETRIC PRESSURE, PRESSURE DROP

FIN AND ANNULUS	TEST NO.	RELATIVE HUMIDITY			STATIC PRESSURE DROP, $(p_1 - p_5)$	BAROMETRIC PRESSURE
		DRY BULB TEMP °F	WET BULB TEMP °F	% HUMD.	INCHES OF WATER	INCHES OF Hg.
I A	1	78.0	73.0	78.0	7.550	29.37
	2	79.0	72.0	72.0	5.125	29.37
	3	78.0	72.0	75.0	5.925	29.37
I B	4	70.0	66.0	83.0	3.700	29.43
	5	70.0	66.0	83.0	4.800	29.43
	6	68.0	64.0	82.0	5.500	29.43
	7	73.0	69.0	83.0	6.375	29.43
	8	70.0	66.0	83.0	7.650	29.43
I C	9	79.0	63.0	42.0	2.040	29.40
	10	80.0	65.0	45.0	3.400	29.40
	11	79.0	67.0	54.0	4.450	29.40
	12	78.0	65.0	50.0	5.750	29.40
	13	77.0	65.0	53.0	6.900	29.40
II A	14	80.0	72.5	70.0	3.800	29.40
	15	79.0	72.0	72.0	4.925	29.40
	16	80.0	72.5	70.0	6.150	29.40
	17	79.0	72.0	72.0	7.150	29.40
	18	80.0	73.0	72.0	7.975	29.40
II B	19	74.0	68.0	75.0	2.675	29.20
	20	73.0	67.0	75.0	3.850	29.20
	21	73.0	68.0	78.0	5.000	29.20
	22	74.0	67.0	70.0	5.850	29.20
	23	73.0	67.0	75.0	7.450	29.20
II C	24	77.0	68.5	63.0	1.550	29.57
	25	76.0	67.0	64.0	2.525	29.57
	26	76.0	67.0	64.0	3.600	29.57
	27	76.0	67.0	64.0	4.600	29.57
	28	75.0	66.0	63.0	5.600	29.57
III A	29	72.0	63.0	62.0	2.025	29.43
	30	72.0	64.0	66.0	3.000	29.43
	31	72.0	63.0	62.0	3.950	29.43
	32	70.0	61.0	60.0	5.800	29.43
	33	71.0	63.0	65.0	5.900	29.43
III B	34	80.0	72.0	68.0	1.850	29.45
	35	80.0	72.0	68.0	2.950	29.45
	36	80.0	72.0	68.0	3.255	29.45
	37	79.0	71.5	69.0	3.925	29.45
	38	79.0	72.0	72.0	4.850	29.45
III C	39	76.0	67.0	64.0	1.725	29.44
	40	76.0	67.0	64.0	2.200	29.44
	41	76.0	66.0	60.0	2.950	29.44
	42	76.0	66.0	60.0	4.275	29.44

TABLE NUMBER 2

ANNULUS INSULATION TEMPS, DEGREES F.

FIN AND ANNULUS	TEST NO:	STATION NO. 1		STATION NO. 3		STATION NO. 5	
		TI1	TO1	TI3	TO3	TI5	TO5
I A	1	89.0	83.0	164.0	96.0	259.0	125.0
	2	93.0	84.0	197.0	106.0	320.0	195.0
	3	90.0	84.0	180.0	102.0	292.0	138.0
I B	4	88.0	80.0	168.0	106.0	284.0	130.0
	5	82.0	78.0	150.0	114.0	245.0	124.0
	6	80.0	78.0	138.0	110.0	228.0	110.0
	7	82.0	78.0	136.0	112.0	216.0	116.0
	8	82.0	78.0	136.0	114.0	202.0	114.0
I C	9	89.0	80.0	133.0	91.0	200.0	114.0
	10	85.0	79.0	119.0	86.0	173.0	104.0
	11	82.0	78.0	112.0	84.0	160.0	100.0
	12	81.0	78.0	107.0	83.0	149.0	94.0
	13	78.0	77.0	104.0	80.0	142.0	90.0
II A	14	99.0	87.0	179.0	106.0	302.0	140.0
	15	93.0	84.0	154.0	97.0	257.0	126.0
	16	91.0	83.0	147.0	94.0	242.0	120.0
	17	88.0	83.0	136.0	92.0	221.0	115.0
	18	89.0	83.0	134.0	90.0	215.0	112.0
II B	19	85.0	74.0	130.0	85.0	209.0	106.0
	20	82.0	73.0	118.0	81.0	180.0	100.0
	21	82.0	73.0	112.0	82.0	164.0	96.0
	22	78.0	75.0	107.0	80.0	151.0	93.0
	23	80.0	76.0	105.0	80.0	145.0	92.0
II C	24	89.0	78.0	128.0	89.0	194.0	108.0
	25	82.0	78.0	114.0	84.0	162.0	97.0
	26	82.0	78.0	109.0	84.0	149.0	97.0
	27	82.0	78.0	105.0	83.0	141.0	93.0
	28	82.0	77.0	103.0	82.0	138.0	89.0
III A	29	91.0	78.0	160.0	94.0	196.0	108.0
	30	86.0	77.0	135.0	89.0	165.0	100.0
	31	81.0	75.0	120.0	85.0	146.0	94.0
	32	78.0	75.0	112.0	84.0	136.0	91.0
	33	78.0	75.0	107.0	80.0	128.0	87.0
III B	34	92.0	85.0	125.0	89.0	165.0	103.0
	35	91.0	84.0	118.0	88.0	152.0	100.0
	36	88.0	83.0	112.0	87.0	139.0	97.0
	37	88.0	83.0	109.0	87.0	133.0	96.0
	38	88.0	83.0	107.0	86.0	128.0	92.0
III C	39	81.0	79.0	119.0	87.0	158.0	95.0
	40	87.0	78.0	110.0	85.0	140.0	90.0
	41	82.0	78.0	106.0	85.0	132.0	88.0
	42	82.0	77.0	101.0	83.0	121.0	84.0

TABLE NUMBER 3

AVERAGE AIR TEMPS., DEGREES F.

FIN AND ANNULUS	TEST NO:	STA NO 1 T_{b1}	STA NO 2 T_{b2}	STA NO 4 T_{b4}	STA NO 5 T_{b5}
I A	1	80.0	135.0	241.0	280.0
	2	80.0	149.3	292.2	336.0
	3	80.0	142.3	270.0	312.0
I B	4	76.0	148.0	278.0	322.0
	5	76.0	134.2	256.8	283.0
	6	76.0	129.2	241.5	278.0
	7	78.0	125.0	228.2	250.0
	8	78.0	121.7	211.0	232.0
I C	9	80.0	132.4	222.3	237.0
	10	80.0	119.0	186.0	194.0
	11	80.0	113.9	166.6	177.0
	12	80.0	106.1	156.1	162.0
	13	80.0	103.1	146.7	155.0
II A	14	84.0	134.4	251.8	284.0
	15	83.0	128.0	215.0	241.0
	16	84.0	121.9	209.1	240.0
	17	83.0	117.0	187.0	221.0
	18	84.0	114.8	192.1	213.0
II B	19	76.0	120.4	233.6	280.0
	20	76.0	112.2	202.7	242.0
	21	76.0	107.4	189.2	221.0
	22	76.0	102.1	173.8	200.0
	23	76.0	100.8	163.6	192.0
II C	24	80.0	130.4	208.3	220.0
	25	80.0	110.5	168.7	178.0
	26	80.0	107.3	153.3	166.0
	27	80.0	103.2	144.5	156.0
	28	80.0	102.7	138.5	151.0
III A	29	76.0	111.0	192.5	218.0
	30	76.0	103.7	167.1	190.0
	31	76.0	100.0	157.3	173.0
	32	76.0	95.9	147.7	165.0
	33	76.0	94.5	136.6	154.0
III B	34	85.0	118.3	196.3	212.0
	35	85.0	113.8	179.1	193.0
	36	85.0	108.0	162.6	176.0
	37	85.0	105.7	153.8	165.0
	38	85.0	104.6	147.4	155.0
III C	39	80.0	111.6	167.7	184.0
	40	80.0	104.8	150.8	160.0
	41	80.0	102.5	139.6	150.0
	42	80.0	99.5	130.0	135.0

TABLE NUMBER 4

FIN-TUBE SURFACE TEMPERATURES, DEGREES F.

FIN AND ANNULUS	TEST NO.	STATION NO. 1			STATION NO. 2		
		TSR1	TSM1	TST1	TSR2	TSM2	TST2
I A	1	162.0	148.0	146.0	247.0	226.0	213.0
	2	183.0	167.0	164.0	278.0	256.0	243.0
	3	173.0	158.0	155.0	263.0	242.0	228.0
I B	4	180.0	166.0	164.0	288.0	268.0	258.0
	5	158.0	151.0	150.0	256.0	245.0	234.0
	6	146.0	139.0	136.0	244.0	230.0	220.0
	7	148.0	136.0	135.0	240.0	221.0	211.0
	8	139.0	130.0	128.0	228.0	207.0	199.0
I C	9	191.0	178.0	174.0	300.0	278.0	264.0
	10	163.0	150.0	148.0	258.0	237.0	223.0
	11	148.0	136.0	135.0	238.0	217.0	203.0
	12	136.0	126.0	125.0	222.0	200.0	187.0
	13	129.0	120.0	119.0	211.0	190.0	176.0
II A	14	207.0	189.0	187.0	275.0	257.0	250.0
	15	191.0	173.0	171.0	252.0	233.0	227.0
	16	185.0	167.0	165.0	244.0	225.0	218.0
	17	175.0	159.0	157.0	231.0	214.0	206.0
	18	173.0	156.0	154.0	227.0	211.0	202.0
II B	19	209.0	192.0	188.0	264.0	246.0	238.0
	20	190.0	172.0	169.0	237.0	219.0	212.0
	21	178.0	162.0	158.0	221.0	203.0	196.0
	22	166.0	150.0	147.0	206.0	188.0	183.0
	23	162.0	146.0	143.0	200.0	182.0	176.0
II C	24	238.0	212.0	208.0	278.0	260.0	254.0
	25	195.0	178.0	176.0	236.0	217.0	211.0
	26	181.0	165.0	162.0	216.0	199.0	193.0
	27	171.0	156.0	154.0	204.0	186.0	180.0
	28	165.0	152.0	148.0	196.0	178.0	172.0
III A	29	243.0	224.0	217.0	306.0	285.0	277.0
	30	218.0	198.0	192.0	273.0	251.0	243.0
	31	201.0	182.0	177.0	252.0	230.0	223.0
	32	190.0	170.0	166.0	237.0	215.0	208.0
	33	181.0	162.0	157.0	225.0	204.0	198.0
III B	34	247.0	228.0	222.0	308.0	288.0	280.0
	35	230.0	211.0	208.0	286.0	266.0	259.0
	36	213.0	194.0	189.0	262.0	241.0	235.0
	37	203.0	184.0	178.0	248.0	227.0	221.0
	38	195.0	175.0	169.0	236.0	216.0	210.0
III C	39	262.0	246.0	236.0	313.0	290.0	283.0
	40	233.0	215.0	209.0	275.0	254.0	248.0
	41	218.0	200.0	194.0	256.0	234.0	227.0
	42	200.0	181.0	175.0	232.0	210.0	203.0

TABLE NUMBER 4 (continued)

FIN-TUBE SURFACE TEMPERATURES, DEGREES F.

FIN AND ANNULUS	TEST NO.	STATION NO. 4			STATION NO. 5		
		TSR4	TSM4	TST4	TSR5	TSM5	TST5
I A	1	333.0	133.0	308.0	340.0	328.0	324.0
	2	390.0	372.0	367.0	403.0	393.0	387.0
	3	362.0	345.0	339.0	376.0	365.0	360.0
I B	4	412.0	387.0	378.0	415.0	401.0	395.0
	5	364.0	349.0	342.0	365.0	350.0	348.0
	6	348.0	333.0	330.0	346.0	332.0	328.0
	7	330.0	312.0	303.0	330.0	316.0	310.0
	8	310.0	290.0	284.0	303.0	294.0	290.0
I C	9	385.0	365.0	357.0	363.0	350.0	344.0
	10	316.0	295.0	288.0	295.0	282.0	277.0
	11	288.0	267.0	258.0	267.0	255.0	250.0
	12	264.0	244.0	237.0	244.0	234.0	227.0
	13	250.0	228.0	222.0	230.0	221.0	213.0
II A	14	394.0	371.0	362.0	395.0	370.0	365.0
	15	352.0	331.0	323.0	352.0	326.0	324.0
	16	338.0	316.0	310.0	337.0	312.0	310.0
	17	316.0	293.0	288.0	314.0	289.0	287.0
	18	309.0	286.0	282.0	307.0	283.0	281.0
II B	19	397.0	375.0	366.0	397.0	375.0	370.0
	20	348.0	327.0	318.0	346.0	322.0	317.0
	21	320.0	300.0	290.0	315.0	294.0	288.0
	22	297.0	275.0	265.0	290.0	268.0	262.0
	23	285.0	261.0	254.0	277.0	254.0	250.0
II C	24	410.0	388.0	378.0	400.0	385.0	378.0
	25	334.0	311.0	303.0	320.0	308.0	300.0
	26	301.0	279.0	271.0	277.0	273.0	267.0
	27	280.0	260.0	252.0	265.0	251.0	246.0
	28	265.0	244.0	236.0	250.0	236.0	231.0
III A	29	399.0	377.0	359.0	383.0	366.0	357.0
	30	354.0	333.0	322.0	337.0	320.0	312.0
	31	324.0	303.0	293.0	306.0	288.0	281.0
	32	303.0	282.0	271.0	286.0	270.0	262.0
	33	286.0	265.0	255.0	269.0	252.0	245.0
III B	34	404.0	282.0	373.0	385.0	367.0	360.0
	35	374.0	353.0	343.0	355.0	337.0	329.0
	36	342.0	319.0	310.0	320.0	305.0	297.0
	37	321.0	300.0	291.0	303.0	284.0	276.0
	38	305.0	283.0	274.0	285.0	267.0	259.0
III C	39	388.0	369.0	361.0	374.0	361.0	353.0
	40	341.0	321.0	313.0	326.0	314.0	307.0
	41	314.0	294.0	287.0	304.0	288.0	280.0
	42	282.0	260.0	253.0	269.0	254.0	247.0

TABLE NUMBER 5

EXPERIMENTAL FIN EFFICIENCIES

FIN AND ANNULUS	TEST NO.	LOCAL FIN EFFICIENCIES STA. NO. 1	STA. NO. 2	STA. NO. 4	STA. NO. 5	AVERAGE FIN EFFICIENCY
I A	1	0.902	0.848	0.864	0.866	0.870
	2	0.907	0.864	0.882	0.880	0.883
	3	0.903	0.855	0.875	0.875	0.887
I B	4	0.923	0.892	0.873	0.892	0.895
	5	0.951	0.909	0.897	0.896	0.913
	6	0.928	0.895	0.915	0.867	0.901
	7	0.907	0.873	0.867	0.875	0.880
	8	0.909	0.863	0.903	0.908	0.896
I C	9	0.923	0.892	0.913	0.924	0.913
	10	0.909	0.874	0.892	0.910	0.896
	11	0.904	0.858	0.876	0.905	0.886
	12	0.901	0.849	0.874	0.896	0.880
	13	0.897	0.837	0.864	0.886	0.871
II A	14	0.918	0.911	0.887	0.864	0.895
	15	0.907	0.899	0.903	0.857	0.891
	16	0.900	0.893	0.891	0.860	0.886
	17	0.902	0.890	0.891	0.854	0.884
	18	0.893	0.888	0.884	0.861	0.882
II B	19	0.921	0.909	0.905	0.884	0.905
	20	0.907	0.899	0.896	0.860	0.891
	21	0.901	0.889	0.885	0.856	0.883
	22	0.894	0.889	0.870	0.844	0.874
	23	0.889	0.879	0.872	0.841	0.870
II C	24	0.904	0.918	0.920	0.938	0.920
	25	0.917	0.900	0.906	0.929	0.913
	26	0.905	0.894	0.898	0.954	0.913
	27	0.906	0.880	0.896	0.912	0.899
	28	0.900	0.871	0.885	0.904	0.890
III A	29	0.922	0.925	0.903	0.921	0.918
	30	0.908	0.911	0.914	0.914	0.912
	31	0.904	0.904	0.907	0.906	0.905
	32	0.894	0.897	0.896	0.900	0.897
	33	0.885	0.896	0.896	0.895	0.893
III B	34	0.922	0.926	0.925	0.927	0.925
	35	0.924	0.921	0.920	0.919	0.921
	36	0.906	0.912	0.910	0.920	0.912
	37	0.894	0.905	0.910	0.902	0.902
	38	0.881	0.901	0.901	0.900	0.896
III C	39	0.928	0.925	0.938	0.944	0.934
	40	0.921	0.920	0.926	0.942	0.927
	41	0.913	0.905	0.922	0.922	0.915
	42	0.895	0.890	0.904	0.917	0.902

TABLE NUMBER 6

AIR PROPERTIES AT THE FLOW MEASURING STAND

FIN AND ANNULUS	TEST NO.	WATER DENSITY lb/ft^3	AIR DENSITY lb/ft^3	VELOCITY PRESSURE INCHES H_2O	AIR VELOCITY ft/sec.	AIR MASS FLOW lb/hr.
I A	1	62.20	0.072	0.175	26.8	353.4
	2	62.20	0.072	0.110	21.2	280.2
	3	62.20	0.072	0.130	23.1	304.6
I B	4	62.24	0.072	0.150	24.7	328.9
	5	62.24	0.072	0.210	29.2	389.1
	6	62.24	0.072	0.255	32.2	428.8
	7	62.24	0.072	0.305	35.3	468.0
	8	62.24	0.072	0.380	39.4	522.4
I C	9	62.20	0.072	0.397	40.3	532.6
	10	62.20	0.072	0.700	53.6	707.3
	11	62.20	0.072	0.950	62.4	824.0
	12	62.20	0.072	1.250	71.6	945.2
	13	62.20	0.072	1.485	78.1	1030.2
II A	14	62.26	0.071	0.200	28.7	376.8
	15	62.17	0.071	0.280	34.0	446.0
	16	62.16	0.071	0.340	37.5	490.9
	17	62.17	0.071	0.420	41.6	546.2
	18	62.16	0.071	0.460	43.6	571.1
II B	19	62.24	0.072	0.240	31.4	414.4
	20	62.24	0.072	0.380	39.5	521.4
	21	62.24	0.072	0.520	46.2	610.0
	22	62.24	0.072	0.660	52.0	687.2
	23	62.24	0.072	0.800	57.3	756.6
II C	24	62.20	0.072	0.430	41.9	555.9
	25	62.20	0.072	0.825	58.0	770.1
	26	62.20	0.072	1.215	70.4	934.5
	27	62.20	0.072	1.565	79.9	1060.0
	28	62.20	0.072	1.920	88.5	1174.8
III A	29	62.24	0.072	0.330	36.6	487.8
	30	62.24	0.072	0.511	45.6	607.1
	31	62.24	0.072	0.692	53.1	706.4
	32	62.24	0.072	0.873	59.6	793.5
	33	62.24	0.072	1.072	66.1	879.3
III B	34	62.15	0.071	0.530	46.8	612.9
	35	62.15	0.071	0.690	53.4	699.3
	36	62.15	0.071	0.970	63.3	829.2
	37	62.15	0.071	1.230	71.3	933.7
	38	62.15	0.071	1.540	79.8	1044.8
III C	39	62.20	0.072	0.820	58.0	766.0
	40	62.20	0.072	1.320	73.5	971.9
	41	62.20	0.072	1.840	86.8	1147.5
	42	62.20	0.072	2.830	107.7	1423.2

TABLE NUMBER 7

DIMENSIONAL DATA FOR FIN TUBES AND ANNULI

FIN AND ANNULUS	A_n CROSS-SECTIONAL FREE FLOW AREA ft^2	P_n CROSS-SECTIONAL WETTED PERIMETER OF FIN TUBE AND ANNULUS, ft.	D_E EQUIVALENT DIAMETER ft.	A_F HEAT TRANSFER SURFACE AREA OF FINS ft^2	A_t HEAT TRANSFER SURFACE AREA OF TUBE ft^2
I A	0.057	2.050	0.0112	6.769	1.375
I B	0.070	2.579	0.1091		
I C	0.096	2.710	0.1414		
II A	0.061	2.140	0.1134	5.165	1.433
II B	0.074	2.538	0.1166		
II C	0.099	2.670	0.1492		
III A	0.063	2.187	0.1146	3.889	1.476
III B	0.076	2.439	0.1246		
III C	0.100	2.567	0.1559		

TABLE NUMBER 8

THE AVERAGE HEAT TRANSFER COEFFICIENT (h_m) CALCULATED FROM THE (LMTD) BETWEEN STATION NO. 1 AND STATION NO. 5

FIN AND ANNULUS	TEST NO.	AIR PROPERTIES EVALUATED AT T_M, °F	ΔT_{lm} °F	G MASS VELOCITY lb/hr ft^2	h_m AVERAGE HEAT TRANSFER COEFFICIENT Btu/hr ft^2 °F
⊙ I A	1	230.0	70.6	6201	33.16
	2	264.0	86.1	4916	26.85
	3	250.0	77.8	5345	29.88
⊡ I B	4	267.0	113.9	4672	20.06
	5	251.0	94.2	5528	23.90
	6	236.0	86.4	6091	26.35
	7	233.0	84.5	6648	27.44
	8	212.0	74.4	7421	30.73
◈ I C	9	244.0	129.7	5560	17.35
	10	216.0	98.1	7383	23.30
	11	206.0	83.5	8601	27.66
	12	190.0	71.3	9866	32.58
	13	181.0	63.8	10754	36.73
△ II A	14	269.0	123.4	6208	22.72
	15	231.0	112.3	7347	25.07
	16	227.0	105.0	8088	26.93
	17	202.0	96.7	8999	29.31
	18	200.0	94.0	9408	30.20
◺ II B	19	265.0	141.6	5600	19.65
	20	225.0	124.0	7047	22.74
	21	209.0	112.2	8243	25.29
	22	194.0	100.1	9287	28.59
	23	191.0	96.3	10225	29.82
◺ II C	24	253.0	174.9	5582	15.72
	25	210.0	130.9	7732	21.15
	26	194.0	110.8	9383	24.99
	27	184.0	104.0	10649	26.94
	28	178.0	96.8	11795	29.16
◻ III A	29	248.0	164.6	7781	20.47
	30	222.0	143.3	9682	23.65
	31	205.0	127.4	11267	26.75
	32	193.0	117.4	12655	29.24
	33	183.0	108.7	14024	31.67
◈ III B	34	253.0	173.1	8064	19.39
	35	234.0	156.0	9202	21.49
	36	216.0	138.5	10910	24.48
	37	211.0	129.7	12286	26.35
	38	197.0	120.8	13747	28.43
◈ III C	39	242.0	191.6	7645	17.39
	40	216.0	162.9	9700	20.56
	41	201.0	149.8	11452	22.58
	42	180.0	129.4	14203	26.41

TABLE NUMBER 9

REYNOLDS NO., PRANDTL NO., NUSSELT NO., AND FANNING FRICTION FACTOR BETWEEN STATION NO. 1 AND NO. 5

FIN AND ANNULUS	TEST NO.	Nre	$Npr^{0.4}$	Nnu	$\frac{Nnu}{Npr^{0.4}}$	f FANNING FRICTION FACTOR
I A	1	12867	0.863	196.7	227.9	0.4862
	2	9854	0.861	153.0	177.5	0.5004
	3	10865	0.862	173.0	200.7	0.4991
I B	4	9167	0.861	111.8	129.7	0.3912
	5	11022	0.862	135.8	157.5	0.3706
	6	12333	0.862	152.3	176.6	0.3573
	7	13503	0.862	159.2	184.6	0.3491
	8	15406	0.863	183.0	211.9	0.3460
I C	9	14460	0.862	128.7	149.2	0.2036
	10	19766	0.863	178.8	207.1	0.2000
	11	23272	0.864	214.9	248.8	0.1960
	12	27179	0.864	258.5	298.9	0.1974
	13	29939	0.865	295.0	341.0	0.2022
II A	14	12632	0.861	131.2	152.3	0.2357
	15	15536	0.862	151.5	175.6	0.2301
	16	17174	0.863	163.6	189.5	0.2385
	17	19617	0.864	183.7	212.5	0.2325
	18	20553	0.864	189.7	219.5	0.2379
II B	19	11759	0.861	117.2	136.1	0.2108
	20	15412	0.863	142.3	164.9	0.2028
	21	18334	0.863	161.5	186.9	0.1970
	22	21000	0.864	186.1	215.2	0.1858
	23	23201	0.864	194.9	225.4	0.1961
II C	24	15179	0.862	121.7	141.2	0.1599
	25	21982	0.863	172.6	199.8	0.1445
	26	27149	0.864	208.1	240.7	0.1433
	27	31175	0.865	227.4	262.9	0.1444
	28	34775	0.865	248.2	286.8	0.1446
III A	29	16345	0.862	122.6	142.1	0.0832
	30	20892	0.863	146.1	169.2	0.0826
	31	24751	0.864	168.8	195.4	0.0824
	32	28177	0.864	187.4	216.7	0.0789
	33	31591	0.865	205.7	237.8	0.0822
III B	34	18323	0.862	125.4	145.5	0.0764
	35	21316	0.862	142.2	164.8	0.0770
	36	25752	0.863	165.6	191.8	0.0774
	37	29152	0.863	179.4	207.7	0.0742
	38	33117	0.864	197.0	227.9	0.0743
III C	39	21975	0.862	142.6	165.4	0.1007
	40	28643	0.863	174.0	201.6	0.0828
	41	34359	0.864	194.7	225.3	0.0835
	42	43664	0.865	234.3	270.8	0.0793

TABLE NUMBER 10

THE AVERAGE HEAT TRANSFER COEFFICIENT (h'_m) CALCULATED FROM THE SEGMENTED (LMTD) BETWEEN STATION NO. 1 AND STATION NO. 5, AIR PROPERTIES EVALUATED AT T_M

FIN AND ANNULUS	TEST NO.	$\Delta T'_{lm}$ °F	h'_m Btu/hr ft^2 °F	N_{Re}	$\frac{N'_{Nu}}{N_{Pr}^{.04}}$
I A	1	94.5	24.78	12867	170.3
	2	106.5	21.72	9854	143.5
	3	99.5	23.37	10865	157.0
I B	4	126.0	18.14	9167	117.4
	5	105.5	21.35	11022	140.6
	6	98.5	23.12	12333	155.0
	7	98.3	24.44	13503	164.3
	8	62.5	24.86	15406	171.4
I C	9	151.0	14.91	14460	128.2
	10	121.5	18.83	19766	167.3
	11	109.3	21.33	23272	190.1
	12	98.7	23.54	27179	216.1
	13	92.0	25.48	29939	236.5
II A	14	136.2	20.59	12632	138.1
	15	128.7	21.89	15536	153.3
	16	119.5	23.68	17174	166.7
	17	114.8	24.78	19617	179.6
	18	109.2	26.02	20553	189.1
II B	19	146.5	19.00	11759	131.6
	20	129.0	21.86	15412	158.5
	21	116.3	24.42	18334	180.4
	22	107.5	26.65	21000	200.6
	23	104.5	27.51	23201	207.9
II C	24	172.0	15.99	15179	143.6
	25	140.5	19.71	21982	186.2
	26	122.5	22.61	27149	217.8
	27	114.5	24.59	31175	240.0
	28	105.0	26.90	34775	264.6
III A	29	193.0	17.46	16345	121.2
	30	170.0	19.94	20892	142.7
	31	152.3	22.39	24751	163.5
	32	141.5	24.26	28177	179.8
	33	133.0	25.89	31591	194.4
III B	34	191.5	17.52	18323	131.5
	35	176.5	19.08	21316	146.3
	36	160.7	21.11	25752	165.4
	37	148.0	23.10	29152	182.1
	38	138.5	24.80	33117	198.8
III C	39	204.0	16.34	21975	155.4
	40	175.5	19.09	28645	187.1
	41	160.0	21.15	34359	211.1
	42	138.5	24.68	43664	253.1

SAMPLE CALCULATIONS

The following set of sample calculations are based on the data of Test No. 15, fin tubeII, annulus A. Fortran Program No. 1 took the appropriate input data and computed numerical values for the Reynolds Number, Prandtl Number, Nusselt Number, and the Fanning friction factor.

1. The density of the air at the flow measuring station was calculated from the relation:

$$\rho = \frac{P}{TR} \qquad \text{Eq. (A-1)}$$

A correction factor for the barometric pressure was also included.

$$\rho = \frac{\left[\frac{29.40}{29.92}\right] 14.69 \times 144.0}{(83.0 + 460.0)(53.3)} = 0.071 \text{ lb/ft}^3$$

2. The average velocity of the air at the flow measuring stand was calculated from the relation:

$$V_m = \sqrt{2g\, C\, (\Delta P/12)\left[\frac{\rho_{H_2O}}{\rho_{AIR}} - 1\right]} \qquad \text{Eq. (A-2)}$$

where C = 0.89 from experimental data

$$V_m = \sqrt{2\,(32.2)\,(0.89)\,(0.175/12)\left[\frac{62.20}{0.071} - 1\right]}$$

$$V_m = 34.0 \text{ ft/sec}$$

3. The volumetric flow rate was calculated from the relation:

$$cfs = (V_m)\ (\text{flow area of measuring stand}) \qquad \text{Eq. (A-3)}$$

$$cfs = (34.0)\ (0.05073) = 1.725\ ft^3/sec$$

4. The mass flow rate of air at the flow measuring stand was found from the relation:

$$M = \rho A V_m = \text{Constant} \qquad \text{Eq. (A-4)}$$

$$M = (cfs)\ (\rho)\ (3600\ sec/hr)$$

$$M = (1.725)\ (0.071)\ (3600) = 446\ lb/hr$$

5. The heat lost from the annular test section to the room through the fiberglass insulation between Station No. 1 and No. 5 was calculated from the temperatures on the inner and outer surface of the fiberglass. Since there was a temperature gradient in the axial direction, the average temperature gradient through the fiberglass was calculated by the (LMTD).

$$\Delta T_{insl} = \frac{(T_{I5} - T_{05}) - (T_{I1} - T_{01})}{\ln\left[\frac{(T_{I5} - T_{05})}{(T_{I1} - T_{01})}\right]} \qquad \text{Eq. (A-5)}$$

$$\Delta T_{insl} = \frac{(257 - 126) - (93 - 84)}{\ln\left[\frac{(257 - 126)}{(93 - 84)}\right]} = 45.5^{\circ}F$$

The heat lost from a hollow cylinder of inner radius r_i and outer radius r_o is:

$$Q_{insl} = \frac{2\pi\ L\ k\ \Delta T_{insl}}{\ln\left[\frac{r_o}{r_i}\right]}$$

$$Q_{insl} = \frac{2\pi\,(33.625/12)\,(0.027)\,(45.5)}{\ln\left[\frac{3.250}{2.250}\right]}$$

$$Q_{insl} = 59 \text{ Btu/hr}$$

Since the total heat imput to the heater was 5.0 kilowatts (17063 Btu/hr), the total heat input to the air was:

$$Q_{air} = Q_{total} - Q_{insl} \qquad \text{Eq. (A-7)}$$

$$Q_{air} = 17063 - 59 = 17004 \text{ Btu/hr}$$

Therefore the heat lost to the room was:

$$\frac{17063 - 17004}{17063} = 0.34\%$$

which can be considered negligible.

6. The average heat transfer coefficient (h_m) between Station No. 1 and No. 5, based on the effective heat transfer area was calculated from the following:

$$h_{m_{1-5}} = \frac{Q_{air}}{(A_{tube} + \phi A_{fin})\,(\Delta T_{lm})_{1-5}} \qquad \text{Eq. (A-8)}$$

Since the local heat transfer coefficient (h) varied in the axial direction, the fin efficiency (ϕ) also varied. Therefore an average value of fin efficiency (ϕ_{ave}) was calculated between

1-5

Station No. 1 and No. 5.

Let ϕ_1 = fin efficiency at Station No. 1, therefore:

$$\phi_1 = \frac{\left[\frac{T_{SR1} + T_{ST1}}{2}\right] - T_{b1}}{T_{SR1} - T_{b1}} \qquad \text{Eq. (A-9)}$$

Bulk temperatures T_{b1}, T_{b2}, T_{b4}, T_{b5} evaluated as shown in Fig. No. 10A

$$\phi_1 = \frac{\left[\frac{191 + 171}{2}\right] - 83}{191 - 83} = 0.907$$

Similarly, let ϕ_2 = fin efficiency at Station No. 2:

$$\phi_2 = \frac{\frac{T_{SR2} + T_{ST2}}{2} - T_{b2}}{T_{SR2} - T_{b2}} \qquad \text{Eq. (A-10)}$$

$$\phi 2 = \frac{\left[\frac{252 + 227}{2}\right] - 128}{252 - 128} = 0.900$$

The fin efficiency midway between Station No. 1 and No. 2 is:

$$\phi_{1.5} = \frac{\phi_1 + \phi_2}{2} \qquad \text{Eq. (A-11)}$$

$$\phi_{1.5} = \frac{0.907 + 0.900}{2} = 0.903$$

Similarly, for Stations No. 2, No. 4, and No. 5:

$$\phi_3 = 0.901, \text{and } \phi_{4.5} = 0.880$$

The average fin efficiency between Station No. 1 and No. 5 is:

$$\phi_{\substack{ave \\ 1-5}} = \phi_{1.5} + \phi_3 + \phi_{4.5} \qquad \text{Eq. (A-12)}$$

$$\phi_{\substack{ave \\ 1-5}} = \frac{0.903 + 0.901 + 0.880}{3} = 0.891$$

The (LMTD) between the air and fin tube heat transfer surface area was determined from Equation (3-8)

$$\Delta T_{lm_{1-5}} = \frac{(352 - 241) - (191 - 83)}{\ln\left[\frac{(352 - 241)}{(191 - 83)}\right]} \doteq 112.3^{\circ}F$$

For fin II, annulus A:

$$A_{tube} = 1.433 \text{ ft}^2$$

$$A_{fin} = 5.165 \text{ ft}^2$$

Therefore:

$$h_{m_{1-5}} = \frac{17004}{(1.433 + (0.891 \times 5.165)\ (112.3)}$$

$$= 25.07 \text{ Btu/hr ft}^2\ ^{\circ}F$$

7. From Figure No. 10 the value of (T_M) was found to be 231°F. The physical properties of the air were:

μ = 0.05365 lb/ft hr

k = 0.01876 Btu/hr ft °F

C_p = 0.241 Btu/lb °F

$\bar{\rho}$ = 0.0574 lb/ft^3

8. For the annular test section the Reynolds Number was defined as:

$$N_{Re} = \frac{\rho V_m D_E}{\mu} \qquad \text{Eq. (A-12)}$$

However, from the continuity equation the air velocity ($\bar{V}_m$) through the annular test section must increase as the density decreases, therefore the velocity of the air where ($\bar{\rho}$) is evaluated at (T_M) is:

$$\bar{V}_m = \frac{M}{\bar{\rho} A_n} \qquad \text{Eq. (A-13)}$$

where $A_n = 0.0607 \text{ ft}^2$

therefore $\bar{V}_m = \dfrac{446}{(0.0574)\ (0.0607)\ (3600 \text{ sec/hr})}$

$= 35.5 \text{ ft/sec} = 128000 \text{ ft/hr}$

Therefore $N_{RE} = \dfrac{(0.0574)\ (128000)\ (0.1134)}{0.05365} = 15536$

The Prandtl number:

$$N_{Pr} = \frac{\mu\ C_p}{k} = \frac{(0.05365)\ (0.2419)}{0.01876} = 0.691$$

The Nusselt Number:

$$N_{Nu} = \frac{h_m\ D_E}{k} = \frac{(25.07)\ (0.1134)}{0.01876} = 151.5$$

and $\dfrac{N_{Nu}}{N_{Pr}^{0.4}} = \dfrac{151.5}{0.862} = 175.6$

The Fanning friction factor:

$$f = \frac{\Delta P\ D_E\ \bar{\rho}\ g_c}{2L\ (G)^2}$$

$$f = \frac{(4.925)\ (5.202)\ (0.1134)\ (0.0574)\ (4.17 \times 10^8)}{2(33.625/12)\ (7347)^2} = 0.2301$$

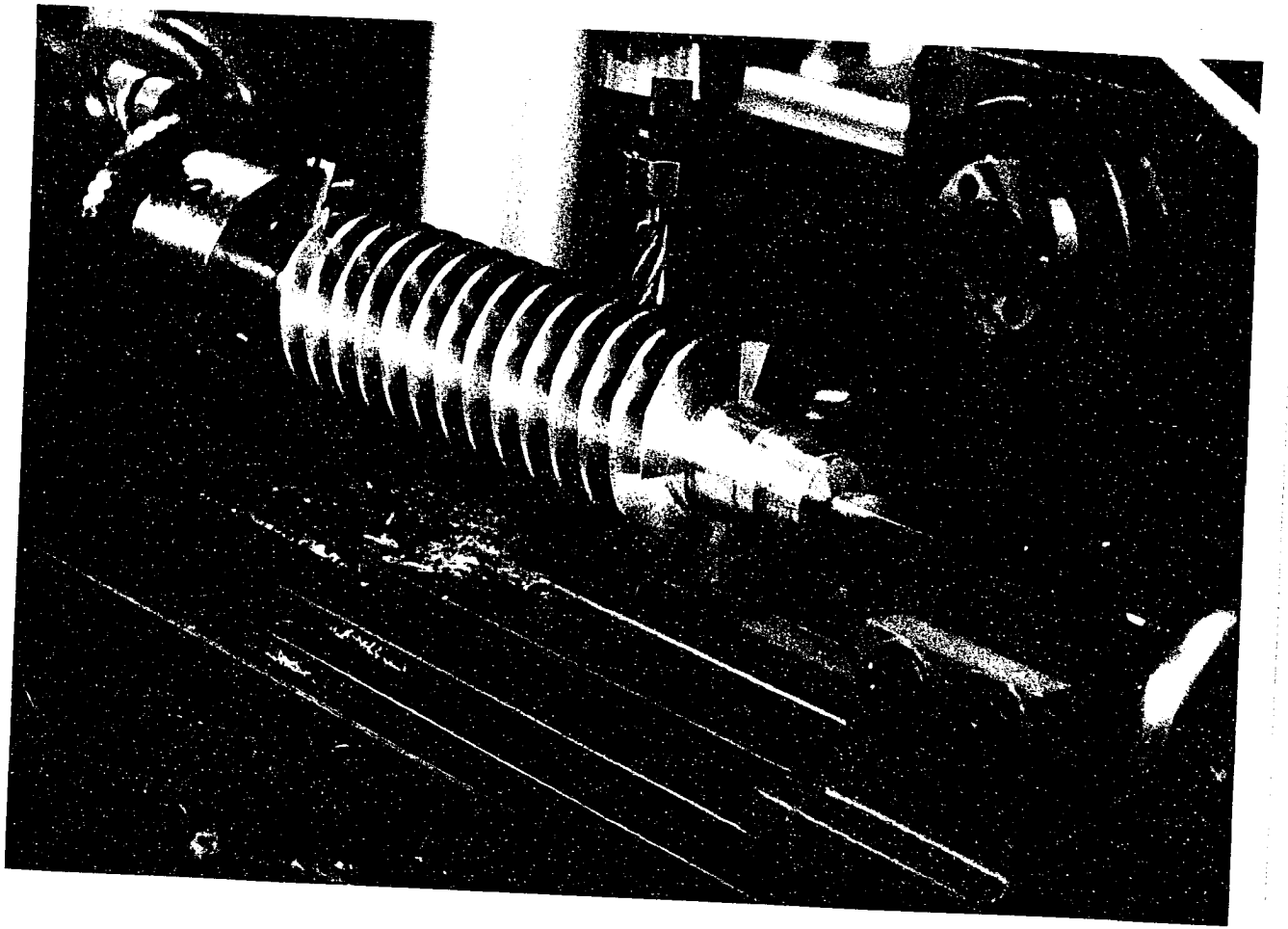

FIGURE NO. 16 PHOTOGRAPH OF FIN TUBES BEING MACHINED ON UNIVERSAL MILLING MACHINE

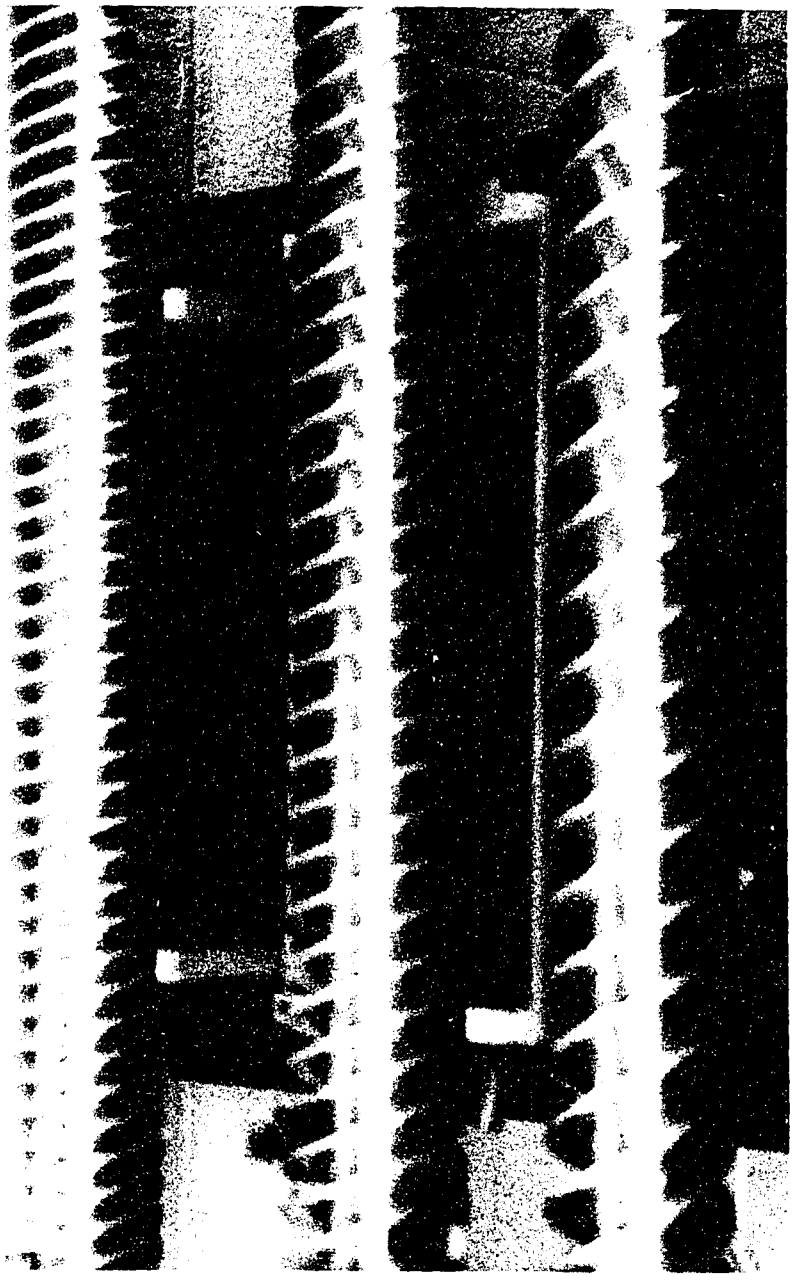

FIGURE NO. 17 PHOTOGRAPH OF FIN TUBES I, II, AND III

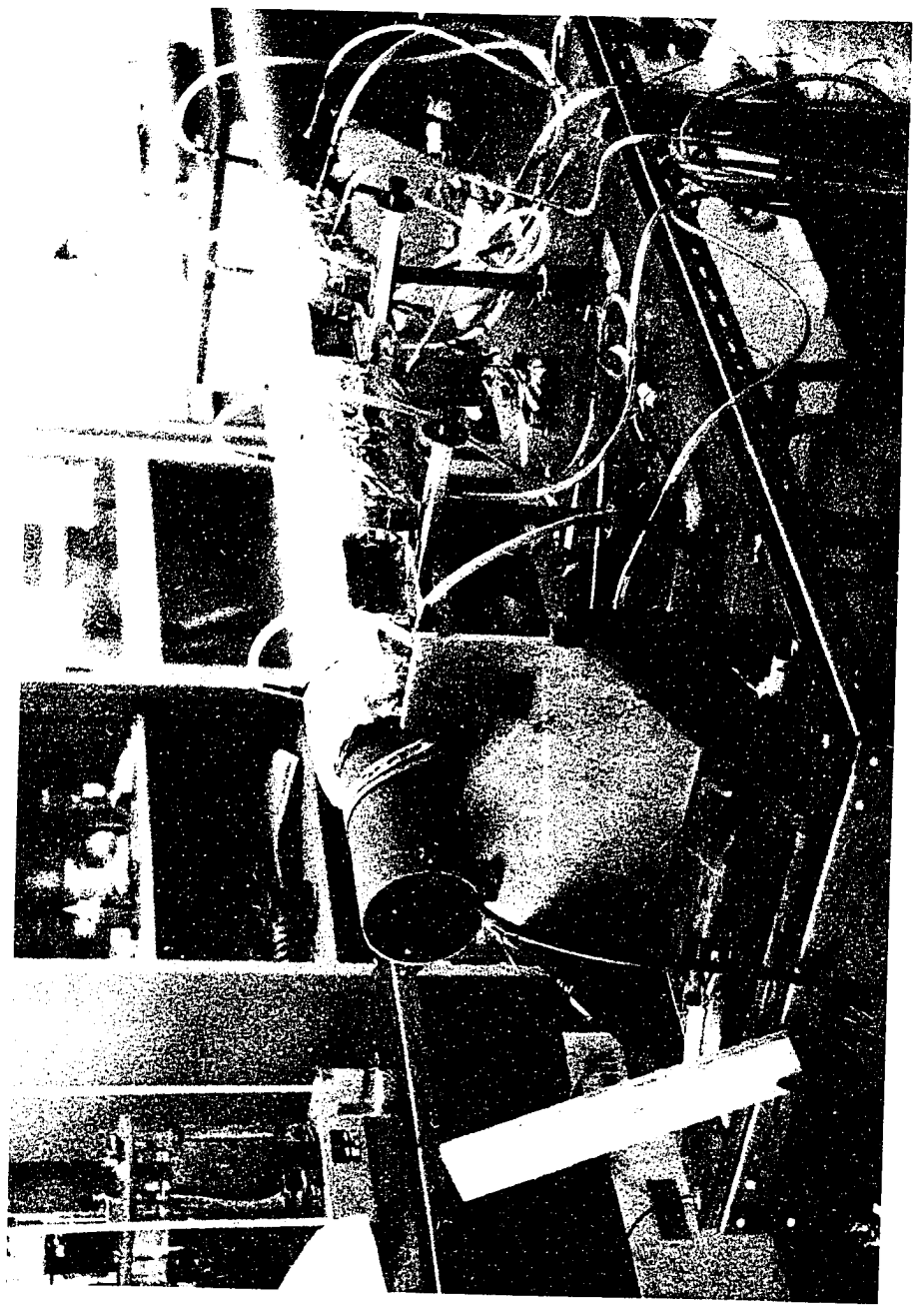

FIGURE NO. 18 PHOTOGRAPH OF TEST SETUP

VITA AUCTORIS

1938 Born in Detroit, Michigan, USA on July 25.

1956 Graduated from Cass Technical High School, Detroit, Michigan.

1962 Received the degree of Bachelor of Science in Mechanical Engineering from Detroit Institute of Technology, Detroit, Michigan.

1966 Currently a candidate for the degree of Master of Applied Science in Mechanical Engineering at the University of Windsor, Windsor, Ontario.